JGR Oceans

RESEARCH ARTICLE
10.1029/2021JC017268

**Key Points:**

- Higher warming rates in open ocean areas than in upwelling areas and general wind stress increases in upwelling areas
- Expansion of desert areas in the open ocean and a general chlorophyll-*a* (Chl-*a*) and productivity decrease, with more pronounced trends in upwelling areas
- The competitive relationship of wind stress and stratification might be responsible for Chl-*a* and productivity trends in upwelling areas

**Supporting Information:**

Supporting Information may be found in the online version of this article.

**Correspondence to:**

E. Fraile-Nuez,
eugenio.fraile@ieo.es

**Citation:**

Siemer, J. P., Machín, F., González-Vega, A., Arrieta, J. M., Gutiérrez-Guerra, M. A., Pérez-Hernández, M. D., et al. (2021). Recent trends in SST, Chl-*a*, productivity and wind stress in upwelling and open ocean areas in the upper Eastern North Atlantic subtropical gyre. *Journal of Geophysical Research: Oceans*, *126*, e2021JC017268. https://doi.org/10.1029/2021JC017268

Received 17 FEB 2021
Accepted 18 JUL 2021



# Recent Trends in SST, Chl-*a*, Productivity and Wind Stress in Upwelling and Open Ocean Areas in the Upper Eastern North Atlantic Subtropical Gyre

**J. P. Siemer[1,3], F. Machín[2], A. González-Vega[3], J. M. Arrieta[3], M. A. Gutiérrez-Guerra[4], M. D. Pérez-Hernández[4], P. Vélez-Belchí[3], A. Hernández-Guerra[4], and E. Fraile-Nuez[3]**

[1]Unversidade do Algarve, Campus de Gambelas, Faro, Portugal, [2]Departamento de Física, Universidad de Las Palmas de Gran Canaria, Las Palmas de Gran Canaria, Spain, [3]Centro Oceanográfico de Canarias, Instituto Español de Oceanografía (IEO), Consejo Superior de Investigaciones Científicas (CSIC), Santa Cruz de Tenerife, Spain, [4]Instituto de Oceanografía y Cambio Global IOCAG, Universidad de Las Palmas de Gran Canaria, Las Palmas de Gran Canaria, Spain

**Abstract** The global upper ocean has been warming during the last decades accompanied with a chlorophyll-*a* (Chl-*a*) and productivity decrease. Whereas subtropical gyres show similar trends, Eastern Boundary Upwelling Systems are thought to increase in productivity due to increased trade winds. This study analyzes recent trends in sea surface temperature (SST), Chl-*a*, net primary production (NPP) and meridional wind stress in the Eastern North Atlantic subtropical gyre (NASE) in order to examine if the global trends can be detected in open ocean and upwelling areas and how the ocean biota responds. Satellite data of such variables of the last 15–40 years were analyzed to calculate mean trends in upwelling areas in the Canary upwelling system and open ocean areas around the Azores, Madeira and the Canary Islands. Our results show significant warming in the area with a maximum of 2.7°C per century for the Azores. Moreover, a general decreasing trend for Chl-*a* and NPP seems to be more evident in the permanent upwelling areas, which will be responsible for a loss of 0.13% of the global NPP per century. Our results also highlight a significant expansion of the oceanic desert area of 10% with an increase in unproductive days of up to 84 days in the last 20 years. The competitive relationship of stratification and wind stress in the Canary upwelling system might be a more plausible explanation for the decrease in Chl-*a* and NPP in upwelling areas linked to the increase in upwelling favorable wind stress and the surface warming.

**Plain Language Summary** The increase in global sea surface temperature (SST) is accompanied with a decrease in chlorophyll-*a* (Chl-*a*) and primary productivity. Microscopic algae called phytoplankton and their pigment Chl-*a* are responsible both for the production of organic material made available for larger animals as food source and the production of oxygen. Different oceanic areas such as the open ocean or coastal so-called upwelling areas in the Eastern North Atlantic Subtropical show characteristic production regimes linked to ocean temperature or wind stress. The main goal of this study was to analyze trends based on satellite data of SST, Chl-*a*, productivity and wind stress in different oceanic areas in order to identify the biological response to the physical forcing. Our study shows that the highly productive upwelling area along Northwest Africa and Western Iberia is warming at a slower pace than open ocean areas around Madeira, the Canary Islands and the Azores where a maximum increase of 2.7°C per century was found. Similarly, the Chl-*a* and the productivity is decreasing faster in the same coastal areas and slower in open ocean areas. If the rate continues it will be responsible for a global loss of 0.13% of the global productivity per century.

## 1. Introduction

The Intergovernmental Panel on Climate Change (IPCC) has identified the role of the ocean as being critical to understand the variability of Earth's climate system (IPCC, 2007, 2013, 2019). A significant increase of global warming trends has been evident in most oceanic regions, both at surface and deep layers (Gouretski & Koltermann, 2007; Johnson & Lyman, 2020; Levitus et al., 2005). Changes in sea surface temperature (SST) have major implications on ocean circulation patterns and ecosystem functioning (Häkkinen

& Rhines, 2004; Parmesan, 2006; Timmermans & Marshall, 2020; Winton et al., 2012). The global ocean warming signal is accompanied with a decreasing trend in chlorophyll-*a* (Chl-*a*) during the last decades (Behrenfeld et al., 2006; Boyce et al., 2010; Signorini et al., 2015; Steinacher et al., 2010). The photic layer is of high scientific concern as at least 50% of the global net primary production (NPP) is oceanic (Lindeman, 1942). Marine phytoplankton not only provides fixed carbon for higher trophic levels and releases oxygen but also constitutes the base of most oceanic food webs (Field, 1998). Global warming effects on phytoplankton and other marine species have already been reported as changes in growth rate, latitudinal habitat displacement and species extinctions (Behrenfeld et al., 2006; Parmesan, 2006; O'Conner et al., 2009; Xiu et al., 2018).

Satellite observations are useful, cost-effective, and time-efficient measures to retrieve and analyze a wide range of different remotely sensed data series of large spatial oceanic areas (Arabi et al., 2020; Davidson et al., 2019; Good et al., 2006). Specific oceanographic areas such as the subtropical gyres and the Eastern Boundary Upwelling Systems (EBUS) exhibit different spatial and temporal trends in SST, Chl-*a*, NPP, and meridional wind (Demarcq, 2009; Gómez-Letona et al., 2017; Polonsky & Serebrennikov, 2018; Polovina et al., 2008). The subtropical gyres are one of the largest marine ecosystems covering 40% of the global surface ocean. Although productivity in these subtropical gyres is generally low, their immense size makes them a large contributor to global primary production. Decreasing Chl-*a* concentrations have been recently reported in all five subtropical gyres (Martinez et al., 2020; Signorini et al., 2015; Vantrepotte & Mélin, 2009). Moreover, it has been reported that the oligotrophic areas in the subtropical gyres are expanding with an accelerating rate (Irwin & Oliver, 2009; Meng et al., 2021; Polovina & et al., 2008). In general, the warming of the surface ocean is expected to increase stratification resulting in limited vertical exchange with lower layers of the ocean and reduced nutrient availability in the photic layer which, in turn, results in low primary production rates (Behrenfeld et al., 2006; Bonino et al., 2019).

EBUS, on the other hand, are highly productive areas contributing to approximately 20% of the global fisheries production despite covering only 1% of the global ocean (Cropper et al., 2014; Santos et al., 2012). During the last decades, the four major upwelling systems (California, Benguela, Peru, and Canary) have shown an increase in SST (Demarcq, 2009; Seabra et al., 2019). Moreover, equatorward upwelling-favorable winds were observed to be increasing their strength in most EBUS (Bakun, 1990; García-Reyes et al., 2015; Sydeman et al., 2014). However, while increasing concentrations of Chl-*a* have been observed in most EBUS, large areas in the Canary upwelling system showed recent decreasing trends in Chl-*a*, NPP (based on ocean color models) and meridional wind (Betancort et al., 2020; Demarcq, 2009; Gómez-Letona et al., 2017). The Eastern North Atlantic subtropical gyre (NASE) comprises the perfect natural habitat to study recent trends in SST, Chl-*a*, NPP, and meridional wind stress in specific oceanographic settings such as upwelling and oligotrophic areas. Although several authors have focused some research on trends in such variables in the NASE detecting a variety of important changes (Arístegui et al., 2009; Cropper et al., 2014; Lemos & Sansó, 2006; Martins et al., 2007; Ould-Dedah et al., 1999; Polonsky & Serebrennikov, 2018; Sambe et al., 2016; Santos et al., 2005, 2012; Taboada & Anadón, 2012), there is a lack of analysis of recent long-term high-resolution time series and how those changes might affect specific sensitive areas in the NASE.

This study presents a combined analysis of remotely sensed data sets of SST, Chl-*a*, NPP, and meridional wind stress and their trends in different oceanographic areas in the NASE over the last 4 decades. Furthermore, the temporal evolution and spatial distribution of productive areas (Chl-$a > 2$ mg m$^{-3}$) and unproductive so-called oceanic desert areas (Chl-$a < 0.07$ mg m$^{-3}$) are examined. Finally, this study aims to evaluate whether the local trends in the Eastern North Atlantic subtropical gyre correspond with those observed globally. We do so by studying satellite-derived estimates of SST, surface Chl-*a*, NPP, and equatorward winds, in two contrasting environments, the Eastern North Atlantic subtropical gyre and its Eastern Boundary Upwelling System.

## 2. Data and Methods

### 2.1. Study Area

A study area covering the NASE (20°N–45°N; 30°W–5°W) was selected for this work (Figure 1). In order to examine spatially linear trends in key regions, eight significant sub-regions were identified: four located

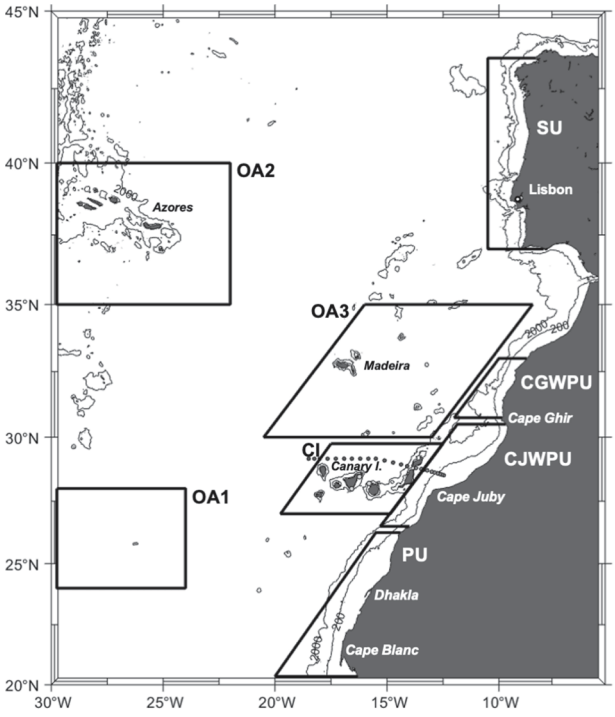


**Figure 1.** Map of the Eastern North Atlantic subtropical gyre (NASE) with areas of interest indicated by polygons. Four polygons are located in upwelling areas: the Permanent Upwelling area (PU), Cape Juby Weak Permanent Upwelling area (CJWPU), Cape Ghir Weak Permanent Upwelling area (CGWPU), and the Seasonal Upwelling area (SU). Four polygons in the open ocean represent the Canary Islands area (CI) and the Open ocean Areas (OA1-3). Locations where upwelling filaments occur (Cape Ghir, Cape Juby, Dhakla, and Cape Blanc) and the Macaronesia Islands (Azores, Madeira, and Canary Islands) are also shown. Dots indicate CTD locations of RaProCan cruises (blue: open ocean and red: upwelling area) and show locations of "Puertos del Estado" buoys (green).

at productive upwelling areas and four at oligotrophic open ocean areas. The upwelling areas were delimited with regards to their upwelling intensity and seasonal behavior as previously described in the literature (Cropper et al., 2014; Gómez-Letona et al., 2017; Van Camp et al., 1991; Wooster et al., 1976). The Permanent Upwelling area (PU) extends from 20°N to 26°N and is characterized by active upwelling throughout the whole year. In the Weak Permanent Upwelling (WPU) area, upwelling occurs also permanently but with lower intensity than in the PU. In both upwelling areas the intensity changes throughout the year, peaking during summer months due to the latitudinal migration of the trade winds (Cropper et al., 2014).

The WPU was divided into two subregions: the Cape Juby Weak Permanent Upwelling area (CJWPU) and the Cape Ghir Weak Permanent Upwelling area (CGWPU). CJWPU covers the area from 26°N to 30°N while the CGWPU stretches from 30°N to 33°N. Upwelling filaments are common features in the permanent and weak permanent upwelling areas and are likely to occur at Cape Ghir, Cape Juby, Dakhla and Cape Blanc due to changes in coastal topography such as headlands (Aristegui et al., 2009; Davenport et al., 2002).

The fourth upwelling area selected is located off the coast of Portugal and Spain (Galicia) between 37°N and 43.5°N. Although the region has been sometimes divided into two subregions in other studies (Arístegui et al., 2009), here it was analyzed as one combined upwelling area. This area was called the Seasonal Upwelling area (SU) because it is characterized by a seasonal upwelling with its peak occurring in the summer months due to changes in atmospheric circulation (Wooster et al., 1976).

In addition, four open ocean areas were selected including three Open ocean Areas (OA1-3) and the oceanic area around the Canary Islands (CI) where complex oceanic circulation patterns such as eddy fields and filaments have been described previously (Fraile-Nuez & Hernández-Guerra, 2006). OA1 is located in the oligotrophic area southwest of the Canary Islands archipelago; OA2 is situated around the Azores; finally, OA3 is the largest area and it stretches from 30°N to 36°N including the region of Madeira.

From a dynamical point of view, the selected areas comprise the Eastern Boundary of the North Atlantic subtropical gyre. The OA2 lies in the path of the Azores Current System mainly by the westward Azores Countercurrent that flows north of the eastward Azores Current (Comas-Rodriguez et al., 2011; Pérez-Hernandez et al., 2013). The OA3 and CI are located in the southwestward flow of the Canary Current parallel to the African coast (Casanova-Masjoan et al., 2020; Hernández-Guerra et al., 2017; Vélez-Belchí et al., 2017). The Canary Current separates from the African coast and feeds the North Equatorial Current that flows to the west through OA1 (Hernández-Guerra et al., 2005; Martínez-Marrero et al., 2008).

### 2.2. Sea Surface Temperature Data

The SST data were provided by the National Oceanic and Atmospheric Administration (NOAA) and produced with their optimum interpolation method applied on remotely sensed satellite data and in situ data from buoys (moored and drifting) and ships (https://www.ncei.noaa.gov/data/sea-surface-temperature-optimum-interpolation/v2/access/avhrr-only/). The satellite instrument used for the SST measurements is the Advanced Very High Resolution Radiometer (AVHRR). The SST in situ data used for the interpolation were obtained from the International Ocean-Atmosphere Data Set (ICOADS). The spatial grid resolution of the analyses is 0.25° and the temporal resolution is daily. Irregularly spaced SST data were transformed into a regular grid (Reynolds, 1988; Reynolds & Marsico, 1993; Reynolds & Smith, 1994; Reynolds et al., 2007). The

original SST time series covers a length of 39 years, from 1981 to 2019. Since the year 1981 is incomplete, the final time series were adjusted to start on January 1, 1982 and end on December 31, 2019 (38 years). Additionally, for each polygon, the days per year when the SST values are above its mean were counted.

Regional validation of the remote sensing SST record provided by NOAA was carried out for this study using independent in-situ data sets from those assimilated on the reanalysis of Reynolds et al. (2007). The comparison between in-situ and satellite measurements was made both for the open ocean and the upwelling area taking into account that lower sensibility has been reported near the coast (Meneghesso et al., 2020). The slope coefficients of the linear regression of both areas are statistically significative (0.8412 and 0.6186, respectively), allowing us to proceed using satellite data on the analysis (Figures SI1 and SI2).

### 2.3. Chlorophyll-*a* Data

Chl-*a* data were provided by Copernicus Marine Environmental Monitoring Service (CMEMS). The product was based on the Copernicus-GlobColour processor that merges three algorithms (Garnesson et al., 2019; Gohin et al., 2002; Hu et al., 2012). Different sensors (SeaWIFS, MODIS Aqua, MODIS Terra, MERIS, VIIRS NPP, VIIRS-JPSS1 OLCI-S3A, and S3B) were used to produce the observations. The original 4 km resolution data was re-gridded to 0.25° resolution with daily temporal resolution. The data used correspond to the L4 "cloud free" day and night interpolated product. The original data set covered the period from September 1997 to June 2019 (Garnesson et al., 2019; https://resources.marine.copernicus.eu/). For processing purposes, the time series were set to start on January 1, 1998 and end on December 31, 2018. Additionally, the actual extension of each pixel of the spatial grid was computed taking into account the variation in distance with longitude in order to calculate the productive extension (pixels with Chl-$a$ > 2 mg $m^{-3}$) in upwelling areas (PU, CJWPU, CGWPU, and SU) and the unproductive, so-called desert areas (pixels with Chl-$a$ < 0.07 mg $m^{-3}$) in the open ocean areas (OA1-3). The methodology to obtain the desert area was adapted from that described by Polovina et al. (2008). An additional metric was calculated by counting the number of days per year when the upwelling areas and open ocean areas were productive (days with Chl-$a$ > 2 mg $m^{-3}$) and unproductive (days with Chl-$a$ < 0.07 mg $m^{-3}$) respectively. Chl-$a$ satellite data could not be validated with in situ-data of the RaProCan cruise since no Chl-$a$ samples were available.

### 2.4. Net Primary Production Data

The NPP data were obtained from the carbon-based production model (CbPm) provided by the Oregon State University (http://orca.science.oregonstate.edu/). In contrast to other chlorophyll-based models, the CbPm model is based on organic carbon estimates that take the physiological state of the primary producers into account. The phytoplankton carbon can be computed from an empirical relationship with the particulate backscattering coefficient. The growth rate is calculated from the chlorophyll-to-carbon ratios. Finally, NPP can be deduced from the phytoplankton carbon and the growth rate (Behrenfeld et al., 2006; Westberry, et al., 2008). The raw satellite data are available from MODIS or SeaWiFS. For this work, MODIS data were used since according to Gomez-Letona et al. (2017) MODIS CbPm provided NPP trends with the highest statistical significance in the Canary upwelling system. The temporal resolution was monthly, and the spatial resolution was 1/12°. The original grid was recalculated to the same resolution as SST and Chl-$a$ (0.25°). The data set starts on January 1, 2003 and ends on December 31, 2018.

### 2.5. Wind Data

Wind data were provided together with the CMEMS product. The data were provided as the reprocessed time series of surface wind analyses containing a global 6-hourly averaged field of several variables such as surface wind speed (wind velocities at 10 m), wind zonal component, wind meridional component and associated errors. The variables were presented on a gridded map with a spatial resolution of 0.25°. Optimum interpolation and kriging methods were applied to enable continuous wind speed and direction measurements for the global ocean. The satellite data were derived from the following institutions and sensors: IFREMER (ERS-1 and ERS-2), NASA/JPL (QuikSCAT and RapidScat), EUMETSAT OSI (ASCAT-A and ASCAT-B), CNSA (HY-2A), ISRO (OceanSat-2), and Remote Sensing System (SSM/I SSMIS, and WindSat). A detailed description of data retrieval and processing methods can be found in Bentamy

et al. (2012, 2013, 2016) and Desbiolles et al. (2017). The time series used here were adjusted to start on January 1, 1992 and to end on December 31, 2018. Although only the equatorward wind (negative v-component) is favorable for upwelling, both poleward (positive v-component) and equatorward wind are included in the analysis. The wind direction was almost exclusively equatorward around the whole year in the permanent upwelling areas and from April to October in the seasonal upwelling area (Wooster et al., 1976). Positive values were therefore not removed to maintain a continuous time series without gaps. Both the meridional and zonal wind stress intensity were calculated from the original wind speed. Besides, and in order to obtain the maximum upwelling-favorable with stress, the wind stress data were projected 25° clockwise to the angle of maximum variance at the African upwelling system (PU, CGWPU, and CJWPU).

An additional metric was calculated by counting the number of days when the wind direction was favorable to upwelling at every upwelling region. Notice, that for this purpose, at PU, CJWPU, and CGWPU, data in the range of 210°–270°W and for SU in the range of 240°–300°W were used (counting counterclockwise from the East–0°).

### 2.6. Linear Fits

Robust fit linear regression (Dumouchel & O'brien, 1991; Holland & Welsch, 1977) and simple linear regression (Chatterjee & Hadi, 1986; Draper & Smith, 1981) were used to assess the temporal trends for different variables. Robust fit linear regression was used for Chl-*a* data (Chl-*a* trends, productive and unproductive days trends) since it is less sensitive to outliers (Demarcq, 2009). Simple linear regression was used for the SST, productive and unproductive areas, NPP and meridional wind data. A statistical significance of 95% confidence level was set for the analysis of all variables.

These linear fit methodologies were applied to the anomalies of the different variables which were obtained by subtracting the seasonal mean component from the original time series. The seasonal mean component was obtained as an annual series containing the daily means (monthly for the NPP data) of the data for all the years in the study. Finally, temporal trends were computed using the slope and the intercept of the linear regression of the anomalies of each variable. Anomalies were used for calculating the trends of all variables except for the productive/unproductive days per year and upwelling-favorable wind days per year.

## 3. Results

### 3.1. Sea Surface Temperature Trends

In order to study the recent temporal and spatial variability in the NASE, temporal trends of SST, Chl-*a*, NPP, and meridional wind at four upwelling areas and four open ocean areas were analyzed.

Figure 2a illustrates the spatial distribution of the SST trends (°C $yr^{-1}$) from 1982 to 2019 (38 years) in the NASE. Although the overall spatial variability is clearly marked by positive values in the whole study area (general warming of +0.201°C $dec^{-1}$; $p < 0.05$), some zones in the permanent upwelling areas (PU and CGWPU) show remarkable negative trends. The most intense cooling trend located in the northern part of the PU area (blue area) represents a decadal rate of −0.139°C $dec^{-1}$; $p < 0.05$.

The temporal variability of the temperature anomaly is shown in Figure 2b. The temperature anomalies in all the analyzed areas exhibit a similar distribution with time. All the time series show an increasing tendency from 1982 to 2019. However, the magnitude of these increases varies for each area (Table 1). Warming trends in the open ocean are generally steeper than in the upwelling areas (Figure 2a; Table 1). OA2 showed the maximum SST increase with a rate of +0.269°C $dec^{-1}$, doubling that observed in CI, OA1, and OA3 which showed comparable warming rates. Some parts of the upwelling areas showed a remarkable cooling tendency but the overall trends in the upwelling areas were also positive but warming was much slower as compared to the open ocean areas. Among the upwelling areas, SU showed the fastest warming ratio, +0.139°C $dec^{-1}$, followed by CJWPU with a value of +0.114°C $dec^{-1}$. Relatively lower warming rates were found in PU and CGWPU, the latter presenting the lowest SST increase with +0.066°C $dec^{-1}$. It is noticeable that the lowest trends were found in areas where cooling areas are present (Figure 2a). All the SST trends were significant with *p*-values <0.05 (Table 1).

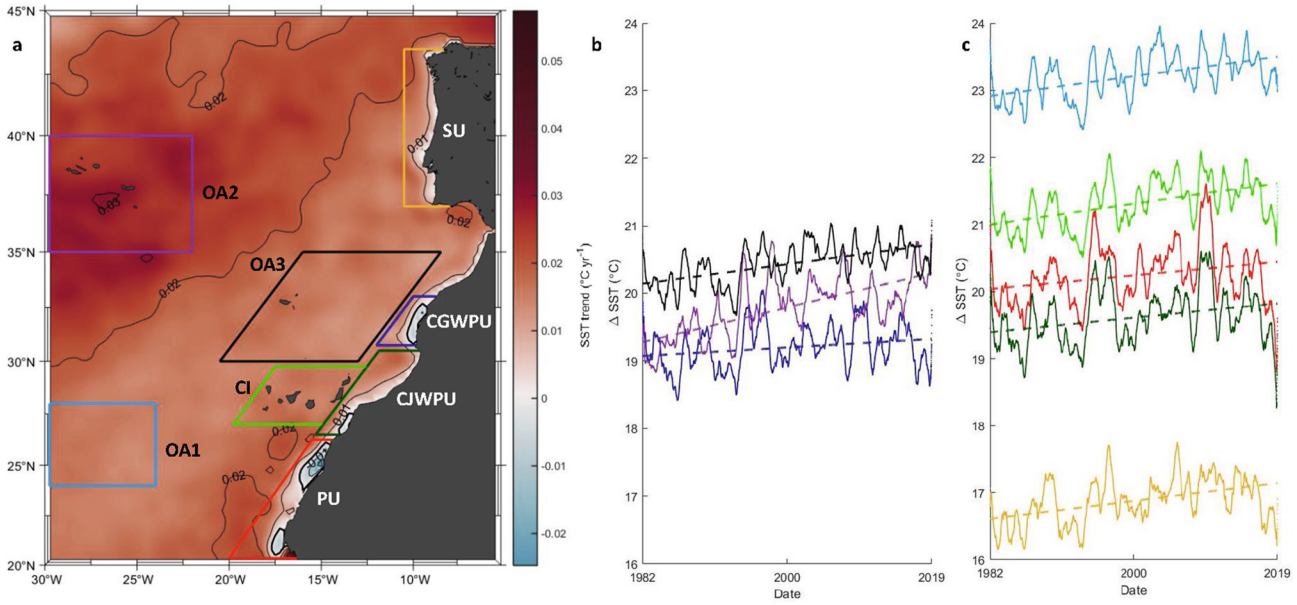


**Figure 2.** (a) Spatial distribution of the sea surface temperature (SST) trend (°C $yr^{-1}$) from 1982 to 2019 in the NASE. The eight polygons show the study areas: four upwelling areas (PU, CJWPU, CGWPU, and SU) and four open ocean areas (CI, OA1-3). Red/blue colors indicate positive/negative SST trend values, respectively. (b) and (c) Smoothed time series (365-days moving average) of the temporal variability of the temperature anomaly as the result of the sum of the temperature anomaly and the mean value of the seasonal SST for CGWPU, OA2, and OA3 in (b) and PU, CJWPU, SU, CI, and OA1 in (c) from 1982 to 2019. The trend for each area is indicated by a dashed line. The y-intercept of the regression line and the y-axis represents the seasonal mean. The colors for each anomaly and trend correspond to the colors of the polygons in (a).

SST trends were also assessed for a shorter time period (27 years from 1992 to 2018 as for the wind data time series). The warming rates from 1992 to 2018 are less intense compared to the warming rates evaluated over the longer time period. However, the general feature of more intense warming in the open ocean, with OA2 having the maximum SST increase of 0.162°C $dec^{-1}$ and less intense warming rates in upwelling areas is still present. As for the longer time period the permanent upwelling and weak permanent upwelling areas (PU, CJWPU, and CGWPU) show less intense SST increases.

Besides, the number of days when the SST raised above the seasonal mean were counted for each polygon for each year and this index was used as further evidence of warming in open ocean and upwelling areas. As expected, all areas exhibited positive rates indicating that the number of days per year when SST values rose above the mean has increased (Table SI1). In fact, all areas show increases in the range of 4–10 days $dec^{-1}$ meaning that those areas have become warmer for 16–40 days over the last 40 years. In general, values calculated from this approach reflect the SST warming rates having lower increases in upwelling areas (4–6 days $dec^{-1}$) and higher increases in open ocean areas (up to 10 days $dec^{-1}$). It should be noted that trends in the upwelling areas are statistically non-significant.

### 3.2. Chlorophyll-*a* Trends

Remotely sensed Chl-*a* is a commonly used proxy for photosynthetic biomass in the ocean surface, and trends of Chl-*a* have been used to get insights into the temporal changes in the productivity of the upper ocean layer (Demarcq, 2009). For the analysis of Chl-*a* a shorter time period from 1998 to 2018 (21 years) was used than for the SST due to limitations in satellite data availability.

Figure 3a displays the spatial variability of the Chl-*a* trends (mg $m^{-3}$ $yr^{-1}$) in the NASE from 1998 to 2018. Chl-*a* rates of change in the entire NASE were mostly negative and relatively small when observed over the whole analyzed area with a mean value of −0.009 mg $m^{-3}$ $dec^{-1}$. The decrease in Chl-*a* concentrations was more evident in coastal areas, especially in the permanent upwelling.

**Table 1**
*Mean Trends of SST, Chl-a, Productive/Unproductive Area, Productive/Unproductive Days (for Upwelling/Open Ocean Areas, Respectively), NPP, Meridional Wind Stress Intensity and Upwelling Favorable Wind Direction Days of Open Ocean and Upwelling Areas*

| Area | Size ($km^2$) | SST 1982–2019 Trend (°C $yr^{-1}$) | SST 1992–2019 Trend (°C $yr^{-1}$) | Chl-*a* 1998–2018 Trend (mg $m^{-3}$ $yr^{-1}$) | Unproductive area Trend (% $yr^{-1}$) | Productive area Trend (% $yr^{-1}$) | Unproductive days Trend (days $yr^{-1}$) | Productive days Trend (days $yr^{-1}$) | NPP 2003–2018 Trend (mg C $m^{-2}$ $day^{-1}$ $yr^{-1}$) | Wind 1992–2018 Trend (mN $m^{-2}$ $yr^{-1}$) | Wind direction days Trend (days $yr^{-1}$) |
|---|---|---|---|---|---|---|---|---|---|---|---|
| PU | 99,800 | **+0.0105** | **+0.0023** | **−0.0311** | | **−0.4892** | | **−2.8364** | *−4.0961* | **0.1823** | **+1.3834** |
| CJWPU | 39,000 | **+0.0114** | **+0.0056** | **−0.0042** | | **−0.0288** | | *+0.0496* | **−9.1985** | **0.2551** | **+1.0159** |
| CGWPU | 27,000 | **+0.0066** | **+0.0024** | **−0.0017** | | **−0.0199** | | | **−8.4379** | **0.4234** | **+1.4029** |
| SU | 74,700 | **+0.0139** | **+0.009** | *+0.0002* | | **+0.0262** | | | **−2.4389** | **0.3941** | **+1.4695** |
| CI | 115,000 | **+0.0162** | **+0.0141** | *−0.0001* | **+0.0637** | | | | **−5.2170** | | |
| OA1 | 283,000 | **+0.0155** | **+0.0161** | **−0.0002** | **+0.4834** | | **+4.1603** | | **−3.0085** | | |
| OA2 | 386,000 | **+0.0269** | **+0.0162** | **−0.0003** | **+0.2278** | | **+0.8339** | | **−4.0527** | | |
| OA3 | 404,000 | **+0.0151** | **+0.0129** | **+0.0004** | **−0.3291** | | **−1.0698** | | **−4.6776** | | |
| NASE | 7,740,000 | **+0.0210** | | **−0.0009** | | | | | **−3.7163** | | |

*Note*. Values in bold are statistically significant and values in italics are statistically non-significant.
Abbreviations: CGWPU, Cape Ghir Weak Permanent Upwelling area; CI, Canary Islands area; CJWPU, Cape Juby Weak Permanent Upwelling area; NASE, Eastern North Atlantic subtropical gyre; NPP, net primary production; OA, Open ocean Areas; PU, Permanent Upwelling area; SU, Seasonal Upwelling area.

The temporal distribution of the Chl-*a* anomaly and the corresponding trends from 1998 to 2018 are shown in Figure 3b. The trends are less homogeneous than for the SST, showing positive and negative values. Nevertheless, it is easy to identify that PU shows the strongest decrease with a value of −0.311 mg $m^{-3}$ $dec^{-1}$ (Table 1). Negative rates were also detected in the weak permanent upwelling areas (CJWPU and CGWPU), though with less intensity. SU is the only upwelling area showing a slight but not significant ($p > 0.05$) increase in Chl-*a*. The open ocean areas OA1-3 presented relatively slower trends as compared to the upwelling areas. Whereas Chl-*a* in OA1 and OA2 is slightly declining, a small but significant increase in photosynthetic biomass was detected in OA3. Trends were statistically significant ($p < 0.05$) both in the open ocean areas (OA1-3) and in the permanent upwelling areas (PU, CJWPU, and CGWPU).

Similar results were evidenced in the analysis of the productive and unproductive area in the upwelling and open ocean areas, respectively (Table 1). The results are expressed in the change of the productive or the unproductive area in percent referenced to the whole area. That is, how much of the whole area of each polygon is becoming more productive or unproductive per decade. As seen in the Chl-*a* trends, the productive area in the permanent upwelling areas (PU, CJWPU, and CGWPU) decreased while in the seasonal upwelling (SU) there was an increase in the area with higher productivity. It should be noted that the productive area in PU shows the strongest decrease with a rate of −4.89% $dec^{-1}$, more than one order of magnitude lower than the other upwelling areas. In close agreement with the evolution of Chl-*a* concentrations, the unproductive areas in CI, OA1, and OA2 were expanding while OA3 became more productive. Interestingly, the fastest expansion rate was found in OA1 with the unproductive area growing at 4.83% $dec^{-1}$.

An additional metric was calculated to characterize the productivity of the upwelling and the open ocean areas. The highly productive (Chl-*a* > 2 mg $m^{-3}$) or unproductive (Chl-*a* < 0.07 mg $m^{-3}$) days per year were counted and used to compute new linear regressions. The results for the open ocean areas closely follow the previous findings and highlight the strong increase in unproductive days for OA1 with an increasing rate of 42 days $dec^{-1}$. In other words, during the last 2 decades the area OA1 has become unproductive for 84 more days (almost a full season) as compared to 1998. In the upwelling areas, only the PU shows a trend with statistical significance with a decrease in productive days up to 28 days $dec^{-1}$. The other upwelling areas and CI did not contain enough values with either Chl-*a* > 2 mg $m^{-3}$ or Chl-*a* < 0.07 mg $m^{-3}$ respectively, to calculate the change in days per years. Again, this result emphasizes the sharp decrease in highly productive days in PU as compared to the other upwelling areas.

We furthermore examined the productive and unproductive days per season (Table SI1). Assessing the seasonal productive days in the upwelling areas was only possible for PU. Although PU productive days were decreasing during every single season along the time series, the most intense decrease was detected during summer with a yearly rate of −1.157 days (24 days in 21 years). For the open ocean areas, the unproductive days were obtained for spring, summer and fall in OA1, OA2, and OA3. The winter season and the CI area did not provide any results

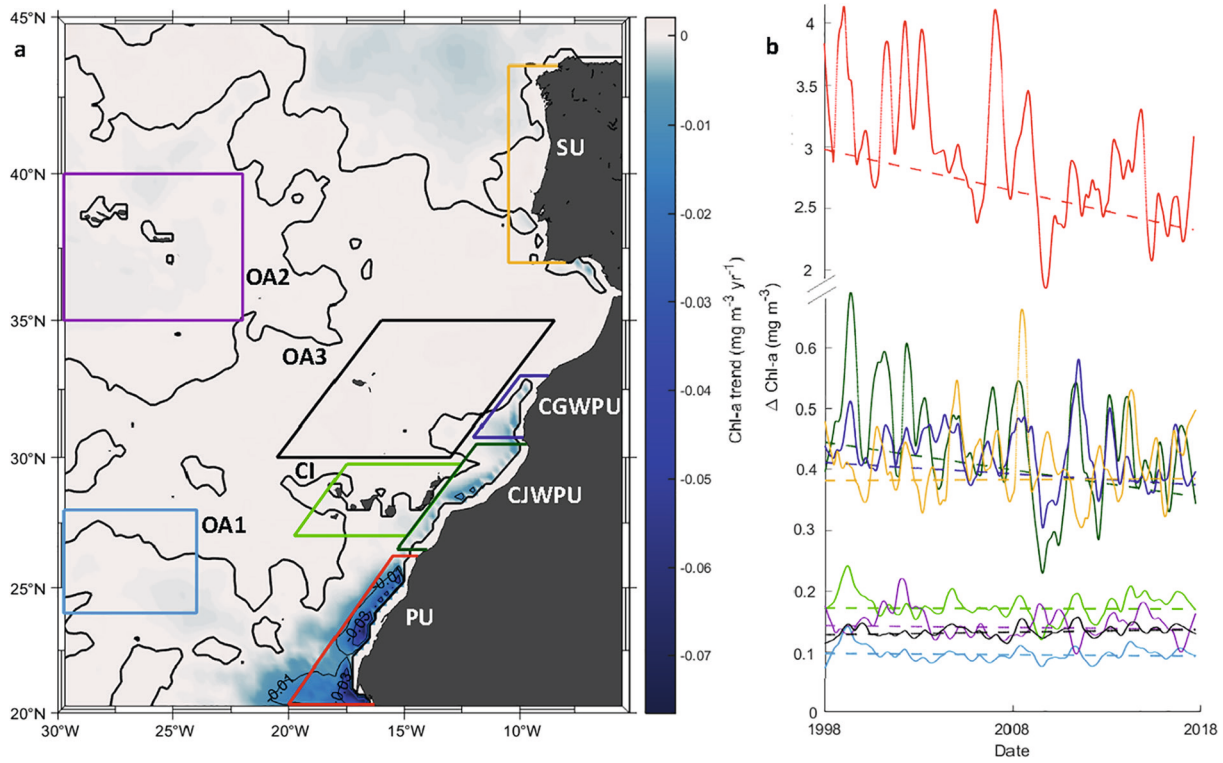


**Figure 3.** (a) Chlorophyll-*a* (Chl-*a*) trends (mg $m^{-3}$ $yr^{-1}$) in the Eastern North Atlantic subtropical gyre (NASE) from 1998 to 2018. The four upwelling areas Permanent Upwelling area (PU), Cape Juby Weak Permanent Upwelling area (CJWPU), Cape Ghir Weak Permanent Upwelling area (CGWPU), and Seasonal Upwelling area (SU) and the four open ocean areas Canary Islands area (CI) and OA1–3 are indicated by different polygons. White areas correspond to trends with values close to 0, and blue tones reflect the intensity of the negative trends. (b) Smoothed time series (365-days moving average) of the Chl-*a* anomaly as the result of the sum and the seasonal mean value and corresponding trends (dashed lines) from 1998 to 2018 for areas shown in (a) (same colors as the polygons). The seasonal mean value is represented by the intercept of the trend with the y-axis.

due to a lack of values. The unproductive days were increasing during each season in OA1 and OA2. For both areas we found the strongest increases during spring followed by summer. Conversely, OA3 was decreasing in unproductive days (hence increasing in productivity) in each season. The most intense decrease was detected during summer with a yearly rate of −0.9242 days (decrease of 19 days in 21 years).

### 3.3. Net Primary Production Trends

Measuring Chl-*a* is the most common proxy used to estimate the NPP of the photic layer. Nevertheless, the physiological state of the phytoplankton is often neglected which results in severe deviations between the Chl-*a* standing stocks and the actual rates of production in marine environments. From the different models designed to produce an estimate of NPP we used the CbPm, which uses the carbon:Chl ratio to derive the NPP (Behrenfeld et al., 2006; Westberry et al., 2008) to complement our Chl-*a* analysis with a more realistic estimate of actual productivity.

Figure 4a shows the spatial distribution of the NPP trends from 2003 to 2018 (15 years) in the NASE. Most of the studied area presents a decrease in NPP, with a mean average of 37.163 mg C $m^{-2}$ $day^{-1}$ $dec^{-1}$. Still, some pixels with increasing values are present. The intensity of the trends (both positive and negative) is highest in coastal areas where the highest production rates were found.

The temporal variability and linear regressions of the NPP anomaly for each area can be seen in Figure 4b. As expected, negative trends were found in all areas of interest. In the upwelling areas, the intensity of the NPP decrease is rather variable. The strongest trend (−91.99 mg C $m^{-2}$ $day^{-1}$ $dec^{-1}$; $p$-value < 0.05) was detected in CJWPU followed by a slightly less intense decrease in CGWPU (−84.38 mg C $m^{-2}$ $dec^{-1}$; $p$-value < 0.05). Values for PU and SU are relatively higher than for CJWPU and CGWPU. SU is the area

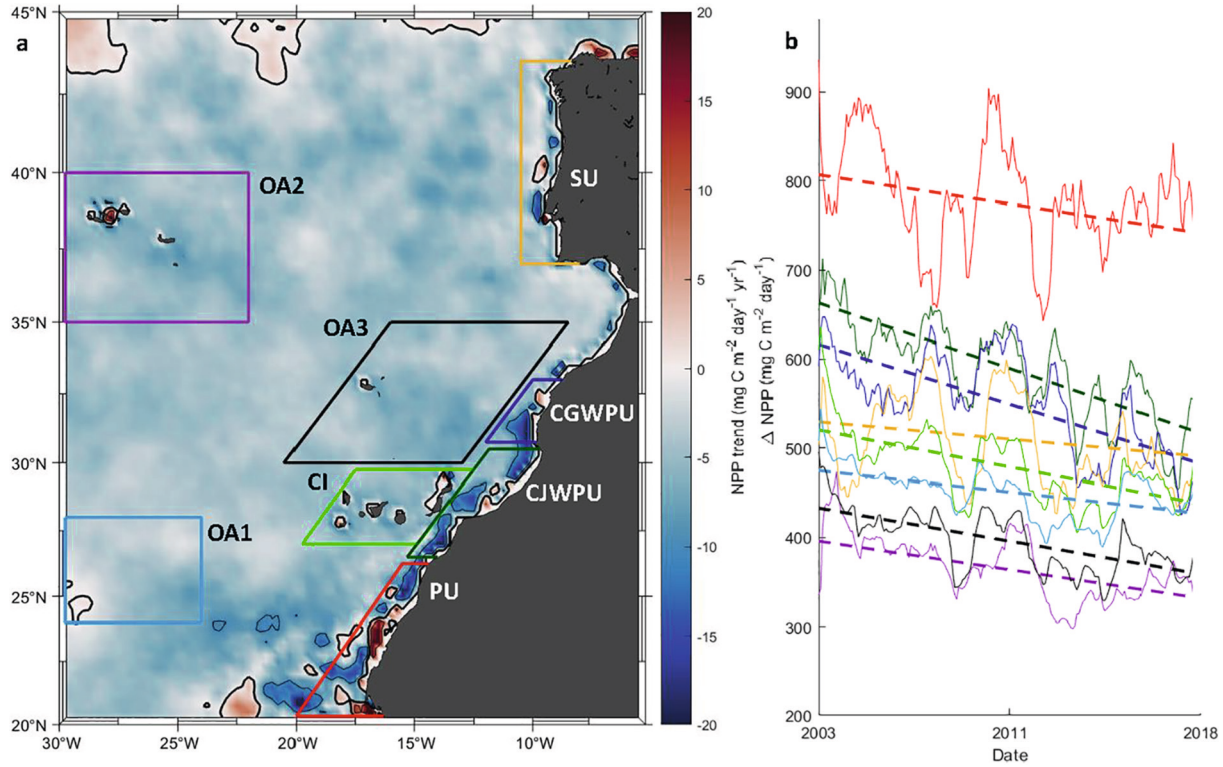


**Figure 4.** (a) Representation of the net primary production (NPP) trends (mg C $m^{-2}$ $day^{-1}$ $dec^{-1}$) from 2003 to 2018 in the Eastern North Atlantic subtropical gyre (NASE). Blue/red areas indicate a decrease/increase in NPP, respectively. Eight areas of interest were selected in upwelling areas (Permanent Upwelling area (PU), Cape Juby Weak Permanent Upwelling area (CJWPU), Cape Ghir Weak Permanent Upwelling area (CGWPU), and Seasonal Upwelling area (SU)) and in open ocean areas (Canary Islands (CI), OA1-3) in order to spatially analyze mean trends. (b) Smoothed time series (12-months moving average) of result of the sum of the NPP anomaly and the seasonal mean value and their regression lines for each area. The mean of each polygon is represented by the intercept of the trend line with the y-axis. The colors correspond to the ones used for the boxes in (a).

with the mildest decrease with a mean value of −24.39 mg C $m^{-2}$ $day^{-1}$ $dec^{-1}$. It is noteworthy that both SU and PU show high p-values as compared to other areas and the trend of PU is statistically non-significant ($p > 0.05$). The open ocean areas (CI and OA1-3) show significant trends but generally not as steep as those in the weak permanent upwelling areas, ranging from approximately −30 mg C $m^{-2}$ $day^{-1}$ $dec^{-1}$ to −52 mg C $m^{-2}$ $day^{-1}$ $dec^{-1}$ ($p$-value $< 0.05$).

To put our results in a global context, we calculated the worldwide rate of NPP by multiplying the original NPP data (mg C $m^{-2}$ $day^{-1}$) by the area of each pixel in the original grid of coordinates to obtain a global rate (mg C $m^{-2}$ $day^{-1}$). Similarly, we calculated the NPP rate of the Canary upwelling system by combining the four upwelling areas (PU, CJWPU, CGWPU, and SU). We obtained the entire time series of NPP rate (2003–2018) and calculated trends following the same approach as with all the variables in this study. In this way, the first and last point of the trend line can be understood as the mean of the NPP rate at the beginning and the end of the time series.

At the beginning of our NPP time series (January 2003), the global rate of NPP was $1.89 \times 10^8$ t C $day^{-1}$, while at the end of the time series (December 2018) this rate was $1.67 \times 10^8$ t C $day^{-1}$, which represents a 11.6% decrease in 15 years. In the Canary upwelling system, the rates were $2.63 \times 10^5$ t C $day^{-1}$ at the beginning and $2.29 \times 10^5$ t C $day^{-1}$ at the end, representing a decrease of 13.2%. These percentages suggest that the NPP rate in the Canary upwelling system is decreasing at a similar pace as the global NPP. Furthermore, the loss in the Canary upwelling system in 15 years ($0.34 \times 10^5$ t C $day^{-1}$) represents a decrease of 0.02% respect to the initial global NPP rate ($1.89 \times 10^8$ t C $day^{-1}$ in January 2003). If this trend continues, this would mean that the Canary upwelling system, which represents 0.11% of the global oceanic area, would be responsible for the loss of 0.13% of the global NPP rate per century.

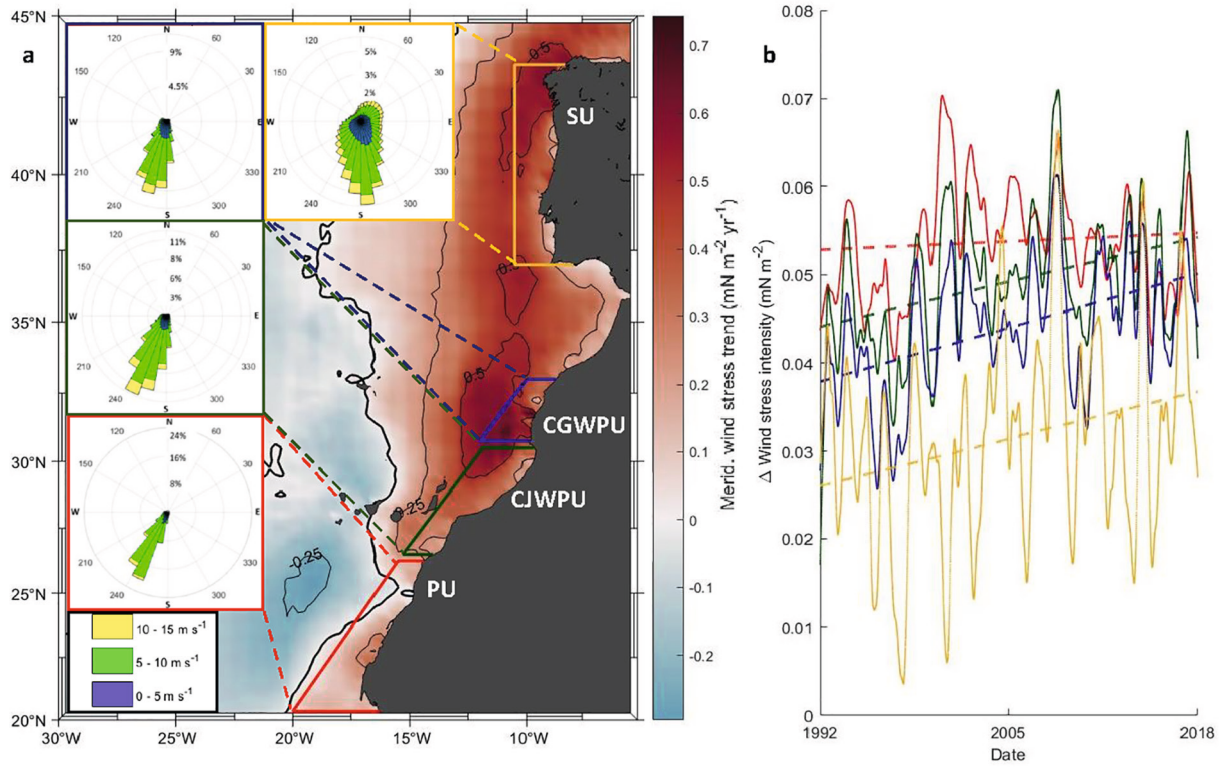


**Figure 5.** (a) Meridional wind stress trend (mN $m^{-2}$ $yr^{-1}$) from 1992 to 2018 in the Eastern North Atlantic subtropical gyre (NASE). Polygons for three permanent upwelling areas (Permanent Upwelling area (PU), Cape Juby Weak Permanent Upwelling area (CJWPU), and Cape Ghir Weak Permanent Upwelling area (CGWPU)) and one seasonal upwelling area (SU) were selected for the analysis of spatial mean trends. Wind roses show the general wind direction and wind speed for each polygon. (b) Smoothed time series (365-days moving average) of the sum of the meridional wind stress anomaly and the seasonal mean value of the meridional wind stress trend of four upwelling areas. The meridional wind stress has been projected for PU, CJWPU and CGWPU by 25° clockwise. Dashed lines represent the trends for each area. The colors of each time series and trends correspond to the polygons and their colors used in (a).

### 3.4. Meridional Wind Trends

The meridional wind stress component was used to analyze the upwelling-favorable wind along the coast of western Iberia and Northwest Africa. In Figure 5a the spatial distribution of the meridional wind stress trends (N $m^{-2}$ $yr^{-1}$) from 1992 to 2018 (27 years) in the NASE is shown. Open ocean areas (CI, OA1-3) are not included in this analysis because the aim is to detect the prevalence of coastal upwelling-favorable wind. Although both increases and decreases in wind stress are present in the whole NASE, positive trends predominate, especially in coastal areas.

In addition, wind roses are displayed to illustrate the general wind direction and wind speed for each upwelling area. The wind direction in PU and the weak permanent upwelling areas (CJWPU and CGWPU) is predominantly south-west. CJWPU and CGWPU show slightly more variation in wind direction and wind speed than PU. The wind direction and wind speed in the SU exhibits greater variability. Nevertheless, the predominant wind direction is to the South.

Figure 5b shows the temporal variability of meridional wind stress anomaly. All four upwelling areas (PU, CJWPU, CGWPU, and SU) show similar temporal variabilities with positive trends of different intensities. The maximum increase in meridional wind stress was found in CGWPU with a mean value of 4.23 mN $m^{-2}$ $dec^{-1}$. CJWPU and SU show relatively lower increases, and PU presents the smallest change in wind speed (1.82 mN $m^{-2}$ $dec^{-1}$). All trends are statistically significant.

As in the case of SST above mean days and the productive and unproductive days we developed another metric to analyze the change in days per year of upwelling favorable wind direction. All upwelling areas show

**Table 2**
*List of SST Trends Related to the Period, Region and Data Sources Found by Published Works in the Literature*

| Study | Results | Period | Region | Data |
|---|---|---|---|---|
| Polovina et al. (2008) | +0.36°C dec$^{-1}$ | 9 years, 1998–2007 | North Atlantic subtropical gyre | NOAA OI SST |
| Demarcq (2009) | +0.35–0.44°C dec$^{-1}$ | 9 years, 1998–2007 | Canary upwelling system | ICOADS, AVHRR Pathfinder version 5.1 |
| Signorini et al. (2015) | +0.18°C dec$^{-1}$ | 15 years, 1998-2013 | North Atlantic subtropical gyre | NOAA OI SST |
| Good et al. (2006) | +0.17–0.18°C dec$^{-1}$ | 19 years, 1985–2004 | Global | AVHRR Pathfinder version 4.1 |
| Gomez-Letona et al. (2017) | Warming and cooling | 21 years, 1993–2014 | Permanent upwelling areas | NOAA OI SST |
| Demarcq (2009) | +0.5°C dec$^{-1}$ | 22 years, 1985–2007 | Canary upwelling system | ICOADS, AVHRR Pathfinder version 5.1 |
| Belkin (2009) | +0.22°C dec$^{-1}$ | 24 years, 1982–2006 | Canary Current | UK Meteorological Office Hadley Centre SST climatology |
| Hansen et al. (2006) | +0.2°C dec$^{-1}$ | 26 years, 1980–2006 | Global | Satellite, ship-based, paleoclimate data |
| Santos et al. (2012) | Warming and cooling | 28 years 1982–2010 | Permanent upwelling areas | AVHRR Pathfinder version 5.2 |
| Casey and Cornillon (2001) | +0.09–0.14°C dec$^{-1}$ | 30 years, 1960–1990 | Global | WOA94, COADS |
| Casey and Cornillon (2001) | +0.05–0.06°C dec$^{-1}$ | 30 years, 1960–1990 | Northeast Atlantic | WOA94, COADS |
| Polonsky and Serebrennikov (2018) | +0.12°C dec$^{-1}$ | 34 years, 1982–2016 | Permanent upwelling areas | NASA PO, DAAC, AVHRR |
| This study | +0.066–0.114°C dec$^{-1}$ | 38 years, 1982–2018 | Permanent upwelling areas | NOAA OI SST V2 |
| This study | +0.139°C dec$^{-1}$ | 38 years, 1982–2018 | SU | NOAA OI SST V2 |
| This study | +0.151–0.269°C dec$^{-1}$ | 38 years, 1982–2018 | NASE, open ocean | NOAA OI SST V2 |
| Padro et al. (2011) | +0.3°C dec$^{-1}$ | 39 years, 1970–2009 | SU | NCEP/NCAR |
| Padro et al. (2011) | +0.21°C dec$^{-1}$ | 39 years, 1970–2009 | Permanent upwelling areas | NCEP/NCAR |
| Ould-Dedah et al. (1999) | Cooling | 42 years, 1946–1988 | Permanent upwelling area | COADS |
| Carson and Harrison (2008) | Warming | 48 years, 1955–2003 | Canary upwelling system | WOD05 |
| Levitus et al. (2000, 2005) | Warming | 50 years, 1950–2000 | Global | World Ocean Database 1998 |
| Baptista et al. (2017) | +0.1–0.2°C dec$^{-1}$ | 60 years, 1950–2010 | SU | ICOADS |
| Lemos and Sansó (2006) | Warming | 100 years, 1900–2000 | SU | World Ocean Database 2001 |

increases in the number of days of upwelling-favorable wind direction in the range of 10–14 days dec$^{-1}$ with a larger effect in the weak permanent upwelling areas (CJWPU and CGWPU).

## 4. Discussion

In order to place our results into a wider context, trends of SST, Chl-*a*, productivity and wind stress are compared to previously published studies. The large variations in time coverage and data sources should be considered. Natural interannual and interdecadal climate variability (e.g., induced by oscillations such as the Atlantic-Multidecadal Oscillation (AMO) or the North Atlantic Oscillation (NAO)) play an important role in the magnitude of trends and can influence the signal of relatively short time periods (Polonsky & Serebrennikov, 2018). Hence, documented long-term trends are the most reliable and most suited ones to compare to our results. In addition, the quality, coverage, and reliability of data sources have changed significantly over the last decades and should also be taken into account. It should also be noted that although Chl-*a* and NPP trends are discussed in one section, both data sets are independent and extracted from two different sources.

### 4.1. Sea Surface Temperature Trends

Our results for the SST are spatially not homogeneous. In fact, the warming in the open ocean is more pronounced than in upwelling areas. Although both higher and lower trends were detected by different authors for different time periods for the open ocean, our results are in good agreement with the literature (Table 2).

Cropper et al. (2014) and Taboada and Anadón (2012) reported general SST increases in the North Atlantic, where warming rates in the open ocean lie in the range of +0.1–0.3°C $dec^{-1}$. Several authors found similar warming rates in the range of +0.18–0.2°C $dec^{-1}$ for the open ocean in the NASE for different time periods between the 1980s and 2000s (Good et al., 2006; Hansen et al., 2006; Signorini et al., 2015). Although the trends of these authors are generally higher than our results, one of the open ocean areas analyzed in the present study, OA2, exhibits an even higher average warming rate (+0.27°C $dec^{-1}$). It has already been emphasized that the temperature is now as high as in the Holocene maximum and it has been warned that a global warming of 1°C higher than the average in 2000 would have adverse effects like sea level rise and species extinctions. An even higher SST warming rate (+0.36°C $dec^{-1}$) for the open ocean than the maximum that we found (+0.27°C $dec^{-1}$) was evidenced by Polovina et al. (2008) in the North Atlantic subtropical gyre from 1998 to 2007. This difference in intensity is probably due to the different length in time periods.

The signal of the trend can easily be affected by climate variability. If the time period selected for the data set is too short, a false signal may be evidenced. For this reason, we tried to assess the trends of the longest records possible. The long-term trends enable both to get more insights into the SST evolution over the last 40 years and may also indicate how the future warming will be affecting the area. However, the time period of the SST time series was also set for 27 years (the same length as the wind data) in order to evaluate if the intensity of the trends over a shorter time period changes significantly. The warming rates for the 27 years' time period show a similar inhomogeneous pattern for open ocean and upwelling areas as the 38 year period. The same differences in warming for upwelling areas and open ocean areas were detected. It should be noted however, that the trends are less intense than for the longer period. Nevertheless, the comparison of both time periods implies that the long-term trend is still present for a shorter time period.

Sambe et al. (2016) found a net warming of the Canary upwelling system and highlight that out of all four EBUS the SST increase in the Canary upwelling system is the strongest one. According to Carson and Harrison (2008), the upper 300 m of the Canary upwelling system have been subject to warming from 1955 to 2003. Warming rates of +0.21°C and +0.22°C were found for periods between 1970–2009 and 1982–2006, respectively (Belkin, 2009; Pardo et al., 2011). Most of the SST increases reported in the literature are higher than the warming rates that we obtained for the permanent upwelling areas. Nevertheless, Polonsky and Serebrennikov (2018) showed that the SST in the active upwelling area increased by +0.4°C from 1982 to 2016 (a rate of +0.12°C $dec^{-1}$). This result reflects the findings of our study. The SST increases in the three permanent upwelling areas vary slightly from the rate they found but are in good agreement with their trend as an average value. Warming was also observed by Lemos and Sansó (2006) in nearshore waters off Iberia. Baptista et al. (2017) analyzed SST variability off Iberia over the last 60 years. The authors found a positive trend in the range of +0.1–0.2°C $dec^{-1}$ which is in good agreement with the results from our study. On the contrary, Pardo et al. (2011) found a higher warming rate from 1970 to 2009 of +0.3°C $dec^{-1}$ for the SU.

Santos et al. (2012) analyzed SST from 1982 to 2010 in the permanent upwelling area and found a warming trend which is increasing southward, noting that some specific areas show surface cooling. They emphasize the spatial differences in open ocean and coastal areas concerning the magnitude of the trends, showing that open ocean areas are subject to higher warming rates. Gómez-Letona et al. (2017) also encountered warming in the permanent upwelling areas that is, higher offshore than in coastal areas. In addition, similar negative trends in coastal areas in the permanent upwelling were detected. They further demonstrate that these areas of cooling are situated at coastal locations where upwelling filaments are common features. Such cooling trends in the permanent upwelling area had already been observed in 1999 by Ould-Dedah et al. (1999), though it has to be noted that they analyzed a different time period (1946–1988).

The differences in warming rates in open ocean and upwelling areas and localized cooling trends might indicate an upwelling intensification as the coastal waters are less warmed due to the cooler upwelled waters (Polonsky & Serebrennikov, 2018). An upwelling intensification would also result in an increase in productivity and surface Chl-*a*. Our results, however, show negative Chl-*a* and NPP trends suggesting that there has rather been a decrease in the upwelling intensity. Both Demarcq (2009) and Santos et al. (2012) suggest that warming in coastal upwelling areas is limited due to upwelled colder waters. This limited warming might be a more reliable explanation for the lower SST trends in the upwelling areas compared to the more pronounced warming in the open ocean.

**Table 3**
*List of Chl-a and NPP Trends Related to the Period, Region, and Data Sources Found by Published Works in the Literature*

| Study | Results | Period | Region | Data |
|---|---|---|---|---|
| Gregg et al. (2005) | Increase | 5 years, 1998–2003 | Global, evident in coastal regions | SeaWiFS Level 3 |
| Gregg et al. (2005) | Decrease | 5 years, 1998–2003 | Subtropical gyres | SeaWiFS Level 3 |
| Behrenfeld et al. (2006)* | Decrease | 9 years, 1997–2006 | Global | VPGM |
| Gomez-Letona et al. (2017) | $-0.025$ mg $m^{-3}$ $dec^{-1}$ | 9 years, 1998–2007 | CJWPU, CGWPU | ESA, SeaWiFS |
| Aristegui et al. (2009) | Decrease | 9 years, 1998–2007 | Canary Current | SeaWiFS Level 3 |
| Demarcq (2009) | $-0.57$ mg $m^{-3}$ $dec^{-1}$ | 9 years, 1998–2007 | Permanent upwelling areas | SeaWiFS Level 3 |
| Demarcq (2009) | Increase | 9 years, 1998–2007 | SU | SeaWiFS Level 3 |
| Vantrepotte and Mélin (2009, 2011) | Decrease | 10 years, 1997–2007 | Subtropical gyres | SeaWiFS |
| Gomez-Letona et al. (2017) | $-0.38$ mg $m^{-3}$ $dec^{-1}$ | 12 years, 2003–2015 | PU | ESA, MODIS |
| Signorini et al. (2015)* | $-73.18$ mg C $m^{-2}$ $day^{-1}$ $dec^{-1}$ | 16 years, 1997–2013 | North Atlantic subtropical gyre | CbPM |
| Gomez-Letona et al. (2017)* | Decrease | 12 years, 2003–2015 | Permanent upwelling areas | CbPM, MODIS |
| Sambe et al. (2016) | $-0.137$ mg $m^{-3}$ $dec^{-1}$ | 15 years, 1997–2012 | Canary Current | NOAA |
| Signorini et al. (2015) | $-0.007$–$0.009$ mg $m^{-3}$ $dec^{-1}$ | 16 years, 1997–2013 | North Atlantic subtropical gyre | SeaWiFS, MODIS |
| Bode et al. (2009) | Decrease | 19 years, 1987–2006 | SU | CPR, Radiales Program |
| This study | $-0.311$–$0.017$ mg $m^{-3}$ $dec^{-1}$ | 21 years, 1982–2018 | Permanent upwelling areas | CMEMS |
| This study | 0.002 mg $m^{-3}$ $dec^{-1}$ | 21 years, 1982–2018 | SU | CMEMS |
| This study | $-0.001$–$+0.004$ mg $m^{-3}$ $dec^{-1}$ | 21 years, 1982–2018 | NASE, open ocean | CMEMS |
| This study* | $-24.39$–$91.99$ mg C $m^{-2}$ $day^{-1}$ $dec^{-1}$ | 21 years, 1982–2018 | NASE | CMEMS |
| Gregg and Conkright (2002) | Decrease | 30 years, 1980–1990 | Global, high latitudes | CZCS, SeaWiFS |
| Gregg and Conkright (2002) | Increase | 30 years, 1980–1990 | Global, low latitudes | CZCS, SeaWiFS |

*Note*. Studies that analyzed NPP trends are marked with an asterisk.

Distribution limits of tropical marine species are believed to shift poleward induced by future warming of the ocean (Verges et al., 2014). The SST increase in the region of the Macaronesian Islands has already resulted both in the arrival of thermophilic species of tropical origin and the geographic expansion of endemic thermophilic species around several islands (Afonso et al., 2013; Brito et al., 2014, 2017). If the SST trend continues it might facilitate future tropicalization and enable the arrival of other tropical species and the population increase of native thermophilic species (Brito et al., 2017). As a consequence, the tropicalization of the environment might also cause the displacement or substitution of species that are adapted to the relatively colder waters along the African shelf (Verges et al., 2014).

### 4.2. Chlorophyll-*a* and Productivity Trends

As in our study, several authors found global Chl-*a* and productivity decreases during the last decades (Table 3). Gregg and Conkright (2002) compared global Chl-*a* variation from 1979 to 1986 (CZCS) and from 1997 to 2000 (SeaWiFS). They identified that global Chl-*a* means were decreasing. Behrenfeld et al. (2006) used NPP (VPGM, chlorophyll-based) data from 1997 until 2006 in order to examine ocean productivity. Similarly, they found a global decrease in productivity. They furthermore emphasized the correlation between stratification and productivity. These authors suggested that enhanced stratification in a warming context suppresses nutrient exchange and productivity due to reduced vertical mixing. In that sense, our results of general decreases in Chl-*a* and productivity are in good agreement with global trends from the literature.

As for the SST trends both the results for Chl-*a* and NPP show significant spatial differences. The trends evidenced in upwelling areas are generally more intense than in open ocean areas. In previous studies, however, authors emphasized the decreasing trends in subtropical gyres. Both Gregg and Conkright (2002)

and Vantrepotte and Mélin (2009, 2011) found a global increase in Chl-*a* for different time periods but Chl-*a* decreases in all five gyres during the time period Vantrepotte and Mélin (2009, 2011) analyzed. Signorini et al. (2015) detected significant negative trends in NPP and Chl-*a* for the North Atlantic subtropical gyre. Although the values of NPP and Chl-*a* are 2–3 times lower than our findings, they are still consistent with the decreases in both NPP and Chl-*a* that we found for the open ocean. Polovina et al. (2008) analyzed the temporal and spatial evolution of the most oligotrophic areas in the subtropical gyres and found supporting evidence of decreasing Chl-*a* concentrations and an expansion of oligotrophic waters. Indeed, the authors detected that the oligotrophic area in the North Atlantic subtropical gyre appeared to be expanding most rapidly (4.3% $yr^{-1}$). This rate is about one order of magnitude higher than the maximum rate of expansion that we found (OA1: 0.4834% $yr^{-1}$). It should be noted however, that Polovina et al. (2008) and Signorini et al. (2015) analyzed the oligotrophic area in the whole subtropical gyre whereas we focused on the eastern part. In fact, the most oligotrophic areas of the North Atlantic subtropical gyre are located rather in the western part of the North Atlantic due to its asymmetry (Munk & Carrier, 1950).

To our knowledge, this is the first time that an analysis based on productive/unproductive days per year to assess the long-term changes in productivity was performed. We detected that the open ocean area OA1 has become almost 90 days more unproductive than 21 years before. This remarkable result, along with the highest expansion rate for this area, suggests that the area is decreasing in productivity at higher rates than other open ocean areas.

In the subtropical gyres the upper ocean is re-stratifying during summer months with shallow mixed-layer depth and limited phytoplankton production that is reduced to ecosystem nutrient regeneration. Climatological changes in the physical forcing such as surface warming/cooling may significantly alter these processes (Signorini et al., 2015). Our results imply that these changes are already occurring leading to the decreases in both Chl-*a* and NPP and the expansion of the most oligotrophic areas.

Several authors found that the Canary upwelling system has decreased in productivity and Chl-*a* over the last 20 years (Aristegui et al., 2009; Demarcq, 2009; Gomez-Letona et al., 2017; Sambe et al., 2016). Although the negative trends are generally in good agreement with our results, the decreases we found for Chl-*a* are more intense. The Chl-*a* trends Gómez-Letona et al. (2017) found for the PU (−0.378 mg $m^{-3}$ $dec^{-1}$) and the weak permanent upwelling areas (−0.025 mg $m^{-3}$ $dec^{-1}$), on the other hand, are in very good agreement with our results (−0.311 mg $m^{-3}$ $dec^{-1}$ and −0.042 to −0.017 mg $m^{-3}$ $dec^{-1}$). These authors analyzed trends in similar locations as in this study and found both increasing and decreasing Chl-*a* concentrations. The NPP (CbPm, MODIS) trends, however, were exclusively negative as in our results, although our values are generally smaller.

Similarly, the productive area and productive days in the permanent upwelling area are decreasing. Indeed, our results show that the PU has lost about two months of high productivity over the last 21 years and the productive area decreased by 10%. As for the open ocean areas this approach has not been used to assess the productivity change over the last decades. Nonetheless, these results provide supporting evidence for the productivity decrease in the permanent upwelling area.

The Canary upwelling system is a highly valuable large marine ecosystem providing ecosystem services with an estimated amount of US$ 11.7 billion (Interwies & Görlitz, 2013). Pelagic fish species are sensitive to changes in the environmental forcing and the state of the environment. It has been hypothesized that sudden environmental changes in 1997 were responsible for the collapse of the sardine stock in the Canary upwelling system. In the last decades, pelagic fish stocks have already been observed to be declining (Sardine, Sardinella) which might be associated to the decreasing Chl-*a* and productivity trends (Sambe et al., 2016). Our results add more evidence to the forecasted decline in pelagic fish stocks that eventually might affect the resources of millions of people that depend on the fisheries activities in the Canary upwelling system.

### 4.3. Wind Trends

Our results indicate meridional wind stress increases and increases in the days when the wind direction was upwelling favorable. These increases are in alignment with previously published studies and especially the upwelling intensification hypothesis (Table 4). In 1990, Bakun (1990) hypothesized that the upwelling

**Table 4**
*List of Wind Trends Related to the Period, Region, and Data Sources Found by Published Works in the Literature*

| Study | Results | Period | Region | Data |
|---|---|---|---|---|
| Demarcq (2009) | Increase | 7 years, 2000–2007 | SU | Cersat, QuickSCAT |
| | Decrease | 7 years, 2000–2007 | Permanent upwelling areas | Cersat, QuickSCAT |
| This study | Increase | 27 years, 1992–2018 | NASE | CMEMS |
| Bakun (1990) | Increase | ~30 years, 1950s–1980s | EBUS | Wind reports from ships |
| McGregor et al. (2007) | Increase | ~30 years, 1950s–1990s | EBUS, Canary upwelling system | COADS |
| Cropper et al. (2014) | Increase | 31 years, 1981–2012 | Permanent upwelling areas | Stations, TWI, MERRA, 20Cr, CFSR, NCEP-DOE II, ERA-I |
| Polonsky and Serebrennikov (2018) | Increase | 34 years, 1982–2016 | Canary upwelling system | NCEP |
| Pardo et al. (2011) | Decrease | 39 years, 1970–2009 | SU | NCEP/NCAR |
| | Decrease | 39 years, 1970–2009 | Permanent upwelling areas | NCEP/NCAR |
| Narayan et al. (2010) | Increase and decrease | 40 years, 1960–2000 | EBUS, Canary upwelling system | COADS, NCEP/NCAR, ERA-40 |
| Barton et al. (2013) | No significant increase | 40 years, 1960–2000 | Permanent upwelling areas | PFEL, NCEP/NCAR, ECMWF, ICOADS, WASWIND |
| | Decrease | 40 years, 1960–2000 | SU | PFEL, NCEP/NCAR, ECMWF, ICOADS, WASWIND |
| Lemos and Pires (2004) | Decrease | 59 years, 1941–2000 | SU | Meteorological stations |
| Betancort et al. (2020) | Decrease | 79 years, 1948–2017 | Canary Islands | NCEP/NCAR |

favorable winds would intensify under global warming. Briefly, the Bakun hypothesis initiated from the fact that trade winds in all four EBUS (Canary, California, Peru, and Benguela) had increased from the mid-1900s to the 1980s. It was therefore proposed that upwelling in EBUS will be increasing during future global warming scenarios. In fact, the author hypothesized that a global warming scenario with increased $CO_2$ concentrations would reduce night-time cooling and increase daytime warming. Consequently, the temperature difference at land and sea would cause greater pressure gradients leading to intensified alongshore winds and enhanced upwelling.

However, a more recent study of Sydeman et al. (2014) who performed a meta-analysis of wind trends in the literature emphasizes equivocal results for the permanent upwelling area in the Canary upwelling system. Barton et al. (2013) support this discussion by underlining the variations in different data sets and locations (even positive and negative trends for the same location). They therefore conclude no intensification in winds off Northwest Africa.

In contrast to our results, some authors have also evidenced negative wind trends for similar time periods. Pardo et al. (2011) used the NCEP/NCAR data set and found a wind decrease in Iberia and Northwest Africa which is most prominent from 1970 to 2009. Similarly, Betancort et al. (2020) detected a net decrease of up to 1 m $s^{-1}$ in wind intensity north of the Canary Islands from 1948 to 2017 using the same data set. Narayan et al. (2010) detected differences between data sets and concluded that COADS data provided the most reliable results of significant increases in meridional wind stress in all four EBUS (in CCU from 28.5 to 33.5°N). In addition, they argue that the less reliable results derive from the NCEP/NCAR data. Smith et al. (2001) showed that the NCEP/NCAR reanalysis data underestimate the global wind intensity. Narayan et al. (2010) consequently suggested that the underestimation of the wind strength might be the reason for the negative trends.

Several authors have indeed found increases in the meridional wind stress in agreement with our results. Cropper et al. (2014) carried out a more holistic approach to analyze the changes in the wind state of the last decades. They found further evidence of increases in upwelling favorable winds (from oceanic stations; two out of four significant) during summer months from 1981 to 2012. Moreover, they computed the Trade Wind Index (difference of sea level pressure from Azores and Cape Verde) which also suggests an intensification of winds since 1973. They additionally represented the meridional wind trends from several data sets

(MERRA, 20CR, CFSR, NCEP-DOE II, and ERA-I reanalysis) from 1981 to 2012. The pattern of meridional wind trends and the intensity of the trends (up to 0.5 m $s^{-1}$ $dec^{-1}$) are consistent with our results. Polonsky and Serebrennikov (2018) examined the wind intensity (modulus and both zonal and meridional wind components) in Northwest Africa during the last 30 years, also showing an increase in wind intensity for the modulus and both the meridional and zonal components.

Santos et al. (2005) analyzed the Canary upwelling system from 1982 to 2001 and detected decadal shifts in the upwelling intensity. They found that the variability in wind forcing provides reasonable explanations for the shifts in upwelling intensity and their timing. Conversely, our results lead in some extent to contradictory correlations. As suggested by Santos et al. (2005) we would expect a productivity increase in relation to strengthened upwelling-favorable wind stress intensity. Nevertheless, our results show a general decrease in Chl-*a* and productivity and an increase in meridional wind. Moreover, our findings both support and contradict Bakun's hypothesis. On the one hand, the mostly decreasing trends in productivity and Chl-*a* in upwelling areas do not agree with Bakun's upwelling intensification hypothesis. On the other hand, the increases in upwelling favorable wind in Iberia and Northwest Africa upwelling areas support the upwelling intensification hypothesis. Furthermore, the general warming in upwelling areas contrasts with Bakun's hypothesis but is consistent with the decreasing productivity. Interestingly, some specific areas do show cooling trends in the permanent upwelling areas, supporting the upwelling intensification hypothesis.

Bonino et al. (2019) pointed out that both the wind stress and the stratification should be considered in order to evaluate future changes in coastal upwelling. Bakun (1990) did not consider the stratification and other processes that might change the thermocline depth such as coastal trapped waves. Warming in coastal areas increases the stratification and inhibits the vertical nutrient exchange limiting the productivity (Brady et al., 2019; Di Lorenzo et al., 2005; Garcia-Reyes et al., 2015). Coastal trapped waves can also change the water column stratification and cause anomalies affecting the productivity (Bachèlery et al., 2016; Echevin et al., 2014; Pietri et al., 2014; Rykaczewski & Dunne, 2010). In fact, both the wind stress and the stratification are able to amplify or mitigate the upwelling intensity. Consequently, changes in wind stress and stratification might be complementary or competitive for the upwelling intensity in a global warming scenario (Bachèlery et al., 2016; Pietri et al., 2014). Bonino et al. (2019) found that in the Canary upwelling system the stratification and coastal trapped waves seem to have stronger effects on the upwelling intensity than in other EBUS such as the Benguela system where a positive linear relationship exists between the upwelling intensity and the wind stress.

## 5. Conclusions

Our study highlights the differences in warming trends in SST and decreasing Chl-*a* and NPP trends in open ocean areas and upwelling areas. SST trends show significant variations in their magnitude with higher warming trends in open ocean (+0.151 to +0.269°C $dec^{-1}$) than in upwelling areas (+0.066–+0.139°C $dec^{-1}$). The SST above the mean days trends reflect the warming rates observed in the SST trends. One of the more relevant results was evidenced in the open ocean area around the Azores (OA2), where an alarming maximum warming rate of +2.7°C per century was found.

Chl-*a* and NPP, however, show more intense decreases in permanent upwelling areas (Chl-*a*: −0.311–−0.017 mg $m^{-3}$ $dec^{-1}$ and NPP: −91.96–−40.96 mg C $m^{-2}$ $day^{-1}$ $dec^{-1}$) than in the open ocean (Chl-*a*: −0.003–−0.001 mg $m^{-3}$ $dec^{-1}$ and NPP: −52.17–−30.09 mg C $m^{-2}$ $day^{-1}$ $dec^{-1}$) and during the last 15 years, the NPP in the Canary upwelling system is decreasing more rapidly (−13.2%) than the global ocean (−11.6%). If the current pace continues, the Canary upwelling system will contribute with a loss of 0.13% to the global NPP.

In general, warming coincides with decreases in Chl-*a*, productivity, and productive area. Three areas in the permanent and weak permanent upwelling (PU, CJWPU, and CGWPU) and three open ocean areas (CI, OA1 and OA2) show warming trends accompanied with decreasing Chl-*a* and NPP trends.

Besides, the permanent upwelling area (PU) has become 60 days more unproductive and the productive area has shrunken by 10% from 1998 to 2018. The oceanic area around the Azores (OA2) has become 17 days more unproductive and the unproductive area has expanded by approximately 5%. The southernmost open

ocean area (OA1) shows the greatest productivity decrease. The area has become up to 87 days more unproductive than in 1998 and the unproductive areas has expanded by up to 10%. Conversely, the open ocean area around Madeira (OA3) exhibited a Chl-*a* increase (+0.04 mg $m^{-3}$ $dec^{-1}$) accompanied with an increase of the productive days up to 22 days during the last 21 years together with an expansion of the productive area by a +7%.

Increasing trends in the meridional wind stress intensity and the upwelling favorable wind direction (around 40 days more upwelling favorable from 1992 to 2018) lead to contradictory conclusions. Although the increase in meridional wind stress is in agreement with Bakun's upwelling intensification hypothesis, it contrasts with decreases in Chl-*a* and NPP in upwelling areas. Interestingly, there are some specific locations in the permanent upwelling areas that exhibit cooling trends of up to −1.4°C per century coinciding with locations where upwelling filaments are characteristic features. In one of these locations a small area shows increases in productivity. These results would support Bakun's hypothesis as enhanced upwelling forced by increasing winds would lead to a cooling of surface waters and an increase in productivity.

The warming in the open ocean and upwelling areas, however, appears to be in better alignment with the decreases in Chl-*a*, productivity, the expansion of unproductive areas in the open ocean and the decrease of productive area in the upwelling region than the increases in meridional wind stress and upwelling favorable wind direction days. This relationship is supported by findings of other authors that the stratification and coastal trapped waves which have not been considered by Bakun (1990) may have stronger effects on the upwelling intensity (and productivity) in the Canary current upwelling system than the wind stress.

Both stratification and coastal trapped waves may reduce the productivity by limiting vertical exchange of nutrients to the surface. Therefore, the upwelling intensity is regulated by the interplay of wind stress and stratification. This relationship may be either complementary or competitive. In the case of our study, it seems to be rather competitive. We therefore suggest that the general warming of the upwelling system and the resulting enhanced stratification might be the main forcing for the upwelling intensity and serve as a more reliable explanation for the decrease in Chl-*a* and productivity than the increased upwelling favorable wind stress.

These results emphasize even more the complex interplay of wind stress and stratification in upwelling areas and their competitive or complementary consequences which will be especially important in future climate change conditions. Further studies based on more holistic data sources should be carried out to get more insight into the still controversial evolution of the Canary upwelling system during the last decades. Furthermore, longer time series and reliable data of SST, Chl-*a* and productivity should be established and analyzed in order to monitor the behavior of the upper ocean in upwelling and open ocean areas in preparation for future challenges in a climate change context.

## Conflict of Interest

The authors declare no conflicts of interest relevant to this study.

## Data Availability Statement

The data sets that were used for the analysis are publicly available and can be obtained from different institutions. The SST data can be obtained from NOAA (https://www.ncei.noaa.gov/data/sea-surface-temperature-optimum-interpolation/access/avhrr-only/). The Chl-*a* and the wind data were provided by Copernicus (https://resources.marine.copernicus.eu/). The NPP data are available at http://orca.science.oregonstate.edu/ and is associated to the Oregon State University.

**Acknowledgments**
This research was funded by the Spanish Institute of Oceanography (IEO) as part of the RAPROCAN (Radial Profunda de Canarias) Project, the Canary Islands component of the core observational program of IEO, and VULCANA-III (IEO-2018-2020) projects. Siemer J. P., received financial support from an Erasmus grant as a trainee at the Spanish Institute of Oceanography (IEO) in Tenerife to conduct the research for this manuscript.

## References

Afonso, P., Porteiro, F. M., Fontes, J., Tempera, F., Morato, T., Cardigos, F., & Santos, R. S. (2013). New and rare coastal fishes in the Azores islands: Occasional events or tropicalization process? *Journal of Fish Biology*, *83*, 272–294. https://doi.org/10.1111/jfb.12162

Arabi, B., Salama, M. S., Pitarch, J., & Verhoef, W. (2020). Integration of in-situ and multi-sensor satellite observations for long-term water quality monitoring in coastal areas. *Remote Sensing of Environment*, *239*, 1–17. https://doi.org/10.1016/j.rse.2020.111632

Arístegui, J., Barton, E. D., Álvarez-Salgado, X. A., Santos, A. M. P., Figueiras, F. G., Kifani, S., et al. (2009). Sub-regional ecosystem variability in the Canary Current upwelling. *Progress in Oceanography*, *83*, 33–48. https://doi.org/10.1016/j10.1016/j.pocean.2009.07.031

Bachèlery, M.-L., Illig, S., & Dadou, I. (2016). Interannual variability in the South-East Atlantic Ocean, focusing on the Benguela Upwelling System: Remote versus local forcing. *Journal of Geophysical Research: Oceans*, *121*(1), 284–310. https://doi.org/10.1002/2015jc011168

Bakun, A. (1990). Global climate change and intensification of coastal ocean upwelling. *Science*, *247*, 198–201. https://doi.org/10.1126/science.247.4939.198

Baptista, V., Silva, P. L., Relvas, P., & Teodósio, M. A. (2017). Sea surface temperature variability along the Portuguese coast since 1950. *International Journal of Climatology*, *38*, 1145–1160. https://doi.org/10.1002/joc.5231

Barton, E. D., Field, D. B., & Roy, C. (2013). Canary current upwelling: More or less? *Progress in Oceanography*, *116*, 167–178. https://doi.org/10.1016/j.pocean.2013.07.007

Behrenfeld, M. J., O'Malley, R. T., Siegel, D. A., McClain, C. R., Sarmiento, J. L., Feldman, G. C., et al. (2006). Climate-driven trends in contemporary ocean productivity. *Nature*, *444*, 752–755. https://doi.org/10.1038/nature05317

Belkin, I. M. (2009). Rapid warming of large marine ecosystems. *Progress in Oceanography*, *81*, 207–213. https://doi.org/10.1016/j10.1016/j.pocean.2009.04.011

Bentamy, A., Grodsky, S. A., Carton, J. A., Croizé-fillon, D., & Chapron, B. (2012). Matching ASCAT and QuikSCAT winds. *Journal of Geophysical Research*, *117*, 1–15. https://doi.org/10.1029/2011JC007479

Bentamy, A., Grodsky, S. A., Chapron, B., & Carton, J. A. (2013). Compatibility of C- and Ku-band scatterometer winds: ERS-2 and QuikSCAT. *Journal of Marine Systems*, *117*(118), 72–80. https://doi.org/10.1016/j.jmarsys.2013.02.008

Bentamy, A., Grodsky, S. A., & Elyouncha, A. (2016). Homogenization of scatterometer wind retrievals. *International Journal of Climatology*, *37*, 870–889. https://doi.org/10.1002/joc.4746

Betancort, M. N., Marcello, J., Rodríguez Esparragón, D., & Hernández-León, S. (2020). Wind variability in the Canary current during the last 70 years. *Ocean Science Discussions*, *16*, 951–963. https://doi.org/10.5194/os-16-951-2020

Bode, A., Alvarez-Ossorio, M. T., Cabanas, J. M., Miranda, A., & Varela, M. (2009). Recent trends in plankton and upwelling intensity off Galicia (NW Spain). *Progress in Oceanography*, *83*, 342–350. https://doi.org/10.1016/j.pocean.2009.07.025

Bonino, G., Di Lorenzo, E., Masina, S. & Iovino, D. (2019). Interannual to decadal variability within and across the major eastern boundary upwelling systems. *Scientific Reports*, *9*, 19949. https://doi.org/10.1038/s41598-019-56514-8

Boyce, D. G., Lewis, M. R., & Worm, B. (2010). Global phytoplankton decline over the past century. *Nature*, *466*, 591–596. https://doi.org/10.1038/nature09268

Brady, R. X., Lovenduski, N. S., Alexander, M. A., Jacox, M., & Gruber, N. (2019). On the role of climate modes in modulating the air–sea $CO^2$ fluxes in eastern boundary upwelling systems. *Biogeosciences*, *16*(2), 329–346. https://doi.org/10.5194/bg-16-329-2019

Brito, A., Dorta, C., & Falcón, J. M. (2014). First valid record of *Gymnothorax vicinus* (pisces: Muraenidae) for macaronesian ecoregion (Canary Islands): A process of tropicalization? *Revista de la Academia Canaria de Ciencias*, *26*, 71–78.

Brito, A., Moreno-Borges, S., Escánez, A., Falcón, J. M., & Herrera, R. (2017). New records of *Actinopterygian* fishes from the Canary Islands: Tropicalization as the most important driving force increasing fish diversity. *Revista de la Academia Canaria de Ciencias*, *29*, 31–44.

Carson, M., & Harrison, D. E. (2008). Is the upper ocean warming? Comparisons of 50-year trends from different analyses. *Journal of Climate*, *21*, 2259–2268. https://doi.org/10.1175/2007jcli2002.1

Casanova-Masjoan, M., Pérez-Hernández, M. D., Pickart, R. S., Valdimarsson, H., Ólafsdóttir, S. R., Macrander, A., et al. (2020). Alongstream, seasonal and interannual variability of the North Icelandic Irminger Current and East Icelandic Current around Iceland. *Journal of Geophysical Research: Oceans*, *125*, e2020JC016283. https://doi.org/10.1029/2020jc016283

Casey, K. S., & Cornillon, P. (2001). Global and regional sea surface temperature trends. *Journal of Climate*, *14*, 3801–3818. https://doi.org/10.1175/1520-0442(2001)014<3801:GARSST>2.0.CO;2

Chatterjee, S., & Hadi, A. S. (1986). Influential observations, high leverage points, and outliers in linear regression. *Statistical Science*, *1*, 379–393. https://doi.org/10.2307/224613410.1214/ss/1177013630

Comas-Rodríguez, I., Hernández-Guerra, A., Fraile-Nuez, E., Martínez-Marrero, A., Benítez-Barrios, V. M., Pérez-Hernández, M. D., & Vélez-Belchí, P. (2011). The Azores Current System from a meridional section at 24.5°W. *Journal of Geophysical Research*, *116*, C09021. https://doi.org/10.1029/2011jc007129

Cropper, T. E., Hanna, E., & Bigg, G. R. (2014). Spatial and temporal seasonal trends in coastal upwelling off Northwest Africa, 1981-2012. *Deep-Sea Research Part I Oceanographic Research Papers*, *86*, 94–111. https://doi.org/10.1016/j.dsr.2014.01.007

Davenport, R., Neuer, S., Helmke, P., Perez-Marrero, J., & Llinas, O. (2002). Primary productivity in the northern Canary Islands region as inferred from SeaWiFS imagery. *Deep-Sea Research Part II-Topical Studies in Oceanography*, *49*, 3481–3496. https://doi.org/10.1016/s0967-0645(02)00095-4

Davidson, F., Alvera-Azcárate, A., Barth, A., Brassington, G. B., Chassignet, E. P., Clementi, E., & Zu, Z. (2019). Synergies in operational oceanography: The intrinsic need for sustained ocean observations. *Frontiers in Marine Science*, *6*, 1–18. https://doi.org/10.3389/fmars.2019.00450

Demarcq, H. (2009). Trends in primary production, sea surface temperature and wind in upwelling systems (1998-2007). *Progress in Oceanography*, *83*, 376–385. https://doi.org/10.1016/10.1016/j.pocean.2009.07.022

Desbiolles, F., Bentamy, A., Blanke, B., Roy, C., Mestas-nu, A. M., Grodsky, S. A., & Maes, C. (2017). Two decades [1992-2012] of surface wind analyses based on satellite scatterometer observations Fabien. *Journal of Marine Systems*, *168*, 38–56. https://doi.org/10.1016/j.jmarsys.2017.01.003

Di Lorenzo, E., Miller, A. J., Schneider, N., & McWilliams, J. C. (2005). The warming of the California current system: Dynamics and ecosystem implications. *Journal of Physical Oceanography*, *35*, 336–362. https://doi.org/10.1175/JPO10.1175/jpo-2690.1

Draper, N., & Smith, H. (1981). Applied regression analysis (Vol. 2). Wiley. https://doi.org/10.1080/00401706.1999.10485680

Dumouchel, W., & O'brien, F. (1991). Integrating a robust option into a multiple regression computing environment. In *Computer science and statistics: Proceedings of the 21st symposium on the interface*. American Statistical Association. https://doi.org/10.1007/978-1-4613-9154-8_3

Echevin, V., Albert, A., Lévy, M., Graco, M., Aumont, O., Piétri, A., & Garric, G. (2014). Intraseasonal variability of nearshore productivity in the Northern Humboldt Current system: The role of coastal trapped waves. *Continental Shelf Research*, *73*, 14–30. https://doi.org/10.1016/j.csr.2013.11.015

Field, C. B. (1998). Primary production of the biosphere: Integrating terrestrial and oceanic components. *Science*, *4*, 954. https://doi.org/10.1042/bst0040954

Fraile-Nuez, E., & Hernández-Guerra, A. (2006). Wind-driven circulation for the eastern North Atlantic Subtropical Gyre from Argo data. *Geophysical Research Letters*, *33*, L03601. https://doi.org/10.1029/2005gl025122

García-Reyes, M., Sydeman, W. J., Schoeman, D. S., Rykaczewski, R. R., Black, B. A., Smit, A. J., & Bograd, S. J. (2015). Under pressure: Climate change, upwelling, and eastern boundary upwelling ecosystems. *Frontiers in Marine Science*, *2*. https://doi.org/10.3389/fmars.2015.00109

Garnesson, P., Mangin, A., D'Andon, O. F., Demaria, J., & Bretagnon, M. (2019). The CMEMS globcolour chlorophyll a product based on satellite observation: Multi-sensor merging and flagging strategies. *Ocean Science*, *15*, 819–830. https://doi.org/10.5194/os-15-819-2019

Gohin, F., Druon, J. N., & Lampert, L. (2002). A five channel chlorophyll concentration algorithm applied to sea WiFS data processed by SeaDAS in coastal waters. *International Journal of Remote Sensing*, *23*, 1639–1661. https://doi.org/10.1080/01431160110071879

Gómez-Letona, M., Ramos, A. G., Coca, J., & Arístegui, J. (2017). Trends in primary production in the Canary upwelling system - A regional perspective comparing remote sensing models. *Frontiers in Marine Science*, *4*, 1–18. https://doi.org/10.3389/fmars.2017.00370

Good, S. A., Corlett, G. K., Remedios, J. J., Noyes, E. J., & Llewellyn-Jones, D. T. (2006). The global trend in sea surface temperature from 20 years of advanced very high resolution radiometer data. *Journal of Climate*, *20*, 1255–1264. https://doi.org/10.1175/JCLI4049.1

Gouretski, V., & Koltermann, K. P. (2007). How much is the ocean really warming? *Geophysical Research Letters*, *34*, 1–5. https://doi.org/10.1029/2006GL027834

Gregg, W. W., Casey, N. W. & McClain, C. R. (2005). Recent trends in global ocean chlorophyll. *Geophysical Research Letters*, *32*. https://doi.org/10.1029/2004GL021808

Gregg, W. W., & Conkright, M. E. (2002). Decadal changes in global ocean chlorophyll. *Geophysical Research Letters*, *29*, 20–24. https://doi.org/10.1029/2002gl014689

Häkkinen, S., & Rhines, P. B. (2004). Decline of subpolar North Atlantic circulation during the 1990s. *Science*, *304*, 555–559. https://doi.org/10.1126/science.1094917

Hansen, J., Sato, M., Ruedy, R., Lo, K., Lea, D. W., & Medina-Elizade, M. (2006). Global temperature change. *Environmental Science*, *103*, 14288–14293. https://doi.org/10.1073/pnas.0606291103

Hernández-Guerra, A., Espino-Falcón, E., Vélez-Belchí, P., Dolores Pérez-Hernández, M., Martínez-Marrero, A., & Cana, L. (2017). Recirculation of the Canary current in fall 2014. *Journal of Marine Systems*, *174*, 25–39. https://doi.org/10.1016/j.jmarsys.2017.04.002

Hernández-Guerra, A., Fraile-Nuez, E., López-Laatzen, F., Martínez, A., Parrilla, G., & Vélez-Belchí, P. (2005). Canary current and North equatorial current from an inverse box model. *Journal of Geophysical Research*, *110*, C12019. https://doi.org/10.1029/2005jc003032

Holland, P. W., Welsch, R. E. (1977). Robust regression using iteratively reweighted least-squares. *Communications in Statistics - Theory and Methods*, *6*, 813–827. https://doi.org/10.1080/03610927708827533

Hu, C., Lee, Z., & Franz, B. (2012). Chlorophyll a algorithms for oligotrophic oceans: A novel approach based on three-band reflectance difference. *Journal of Geophysical Research*, *117*, 1–25. https://doi.org/10.1029/2011JC007395

Interwies, E., & Görlitz, S. (2013). *Economic and social valuation of the CCLME ecosystem services. Rapport au Groupe de travail socioéconomie et commerce du CCLME*.

IPCC (2007). Climate change 2007: The physical science basis. In S. Solomon, D. Qin, M. Manning, Z. Chen, M. Marquis, K. B. Averyt, et al. (Eds.), *Contribution of working group I to the fourth assessment report of the intergovernmental Panel on climate change*. Cambridge University Press.

IPCC (2013). Summary for policymakers. In T. F. Stocker, D. Qin, G. K. Plattner, M. Tignor, S. K. Allen, J. Boschung, et al. (Eds.), *Climate change 2013: The physical science basis. Contribution of working group I to the fifth assessment report of the intergovernmental Panel on climate change*. Cambridge University Press.

IPCC (2019). Summary for policymakers. In H.-O. Portner, D. C. Roberts, V. Masson- € Delmotte, P. Zhai, M. Tignor, E. Poloczanska, et al. (Eds.), *IPCC special report on the ocean and cryosphere in a changing climate*. World Meteorological Organization.

Irwin, A. J., & Oliver, M. J. (2009). Are ocean deserts getting larger? *Geophysical Research Letters*, *36*, 1–5. https://doi.org/10.1029/2009GL039883

Johnson, G. C., & Lyman, J. M. (2020). Warming trends increasingly dominate global ocean. *Nature Climate Change*, *10*, 757–761. https://doi.org/10.1038/s41558-020-0822-0

Lemos, R. T., & Pires, H. O. (2004). The upwelling regime off the west Portuguese coast, 1941–2000. *International Journal of Climatology*, *24*, 511–524. https://doi.org/10.1002/joc.1009

Lemos, R. T., & Sansó, B. (2006). Spatio-temporal variability of ocean temperature in the Portugal Current system. *Journal of Geophysical Research*, *111*, 1–14. https://doi.org/10.1029/2005JC003051

Levitus, S., Antonov, J., & Boyer, T. (2005). Warming of the world ocean, 1955–2003. *Geophysical Research Letters*, *32*, 1–4. https://doi.org/10.1029/2004GL021592

Levitus, S., Antonov, J. I., Boyer, T. P., & Stephens, C. (2000). Warming of the world ocean. *Science*, *287*, 2225–2229. https://doi.org/10.1126/science.287.5461.2225

Lindeman, R. L. (1942). The trophic-dynamic aspect of ecology. *Ecology*, *23*, 399–417. https://doi.org/10.2307/1930126

Martinez, E., Gorgues, T., Lengaigne, M., Fontana, C., Sauzède, R., Menkes, C., et al. (2020). Reconstructing global chlorophyll-a variations using a non-linear statistical approach. *Frontiers in Marine Science*, *7*, 1–20. https://doi.org/10.3389/fmars.2020.00464

Martínez-Marrero, A., Rodríguez-Santana, A., Hernández-Guerra, A., Fraile-Nuez, E., López-Laatzen, F., Vélez-Belchí, P., & Parrilla, G. (2008). Distribution of water masses and diapycnal mixing in the Cape Verde frontal zone. *Geophysical Research Letters*, *35*, L07609. https://doi.org/10.1029/2008gl033229

Martins, A. M., Amorim, A. S. B., Figueiredo, M. P., Souza, R. J., Mendonça, A. P., Bashmachnikov, I. L., & Carvalho, D. S. (2007). Sea surface temperature (AVHRR, MODIS) and ocean colour (MODIS) seasonal and interannual variability in the Macaronesian islands of Azores, Madeira, and Canaries. In *Remote sensing of the ocean, sea ice, and large water regions* (pp. 6743). SPIE. https://doi.org/10.1117/12.738373

McGregor, H. V., Dima, M., Fischer, H. W., & Mulitza, S. (2007). Rapid 20th-century increase in coastal upwelling off northwest Africa. *Science*, *315*, 637–639. https://doi.org/10.1126/science.1134839

Meneghesso, C., Seabra, R., Broitman, B. R., Wethey, D. S., Burrows, M. T., Chan, B. K. K., et al. (2020). Remotely-sensed L4 SST underestimates the thermal fingerprint of coastal upwelling. *Remote Sensing of Environment*, *237*, 111588. https://doi.org/10.1016/j.rse.2019.111588

Meng, S., Gong, X., Yu, Y., Yao, X., Gong, X., Lu, K., et al. (2021). Strengthend ocean-desert process in the North Pacific over the past two decades. *Environmental Research Letters*, *16*, 1–10. https://doi.org/10.1088/1748-9326/abd96f

Munk, W. H., & Carrier, G. F. (1950). The wind-driven circulation in ocean basins of various shapes. *Tellus*, *2*, 158–167. https://doi.org/10.3402/tellusa.v2i3.8550

Narayan, N., Paul, A., Mulitza, S., & Schulz, M. (2010). Trends in coastal upwelling intensity during the late 20th century. *Ocean Science*, *6*, 815–823. https://doi.org/10.5194/os-6-815-2010

O'Connor, M. I., Piehler, M. F., Leech, D. M., Anton, A., & Bruno, J. F. (2009). Warming and resource availability shift food web structure and metabolism. *PLoS Biology*, *7*, 1–6. https://doi.org/10.1371/journal.pbio.1000178

Ould-Dedah, S., Wiseman, W. J., & Shaw, R. F. (1999). Spatial and temporal trends of sea surface temperature in the northwest African region. *Oceanologica Acta*, *22*, 265–279. https://doi.org/10.1016/S0399-1784(99)80051-6

Pardo, P. C., Padín, X. A., Gilcoto, M., Farina-busto, L., & Pérez, F. F. (2011). Evolution of upwelling systems coupled to the long-term variability in sea surface temperature and Ekman transport. *Climate Research*, *48*, 231–246. https://doi.org/10.3354/cr00989

Parmesan, C. (2006). *Ecological and evolutionary responses to recent climate change* (pp. 637–671). https://doi.org/10.1146/annurev.ecolsys.37.091305.110100

Pérez-Hernández, M. D., Hernández-Guerra, A., Fraile-Nuez, E., Comas-Rodríguez, I., Benítez- Barrios, V. M., Domínguez-Yanez, J. F., & Vélez-Belchí, P. (2013). The source of the Canary current in fall 2009. *Journal of Geophysical Research: Oceans*, *118*, 1–18. https://doi.org/10.1002/jgrc10.1002/jgrc.20227

Pietri, A., Echevin, V., Testor, P., Chaigneau, A., Mortier, L., Grados, C., & Albert, A. (2014). Impact of a coastal-trapped wave on the near-coastal circulation of the Peru upwelling system from glider data. *Journal of Geophysical Research: Oceans*, *119*(3), 2109–2120. https://doi.org/10.1002/2013jc009270

Polonsky, A. B., & Serebrennikov, A. N. (2018). Long-term sea surface temperature trends in the Canary upwelling zone and their causes. *Izvestiya - Atmospheric and Ocean Physics*, *54*, 1062–1067. https://doi.org/10.1134/S0001433818090281

Polovina, J. J., Howell, E. A., & Abecassis, M. (2008). Ocean's least productive waters are expanding. *Geophysical Research Letters*, *35*, 2–6. https://doi.org/10.1029/2007GL031745

Reynolds, R. W. (1988). A real-time global sea surface temperature analysis. *Journal of Climate*, *1*, 75–86. https://doi.org/10.1175/1520-0442(1988)001<0075:artgss>2.0.co;2

Reynolds, R. W., & Marsico, D. C. (1993). An improved real-time global sea surface temperature analysis. *Journal of Climate*, *6*, 114–119. https://doi.org/10.1175/1520-0442(1993)006<0114:airtgs>2.0.co;2

Reynolds, R. W., & Smith, T. M. (1994). Improved global sea surface temperature analyses using optimum interpolation. *Journal of Climate*, *7*, 929–948. https://doi.org/10.1175/1520-0442(1994)007<0929:igssta>2.0.co;2

Reynolds, R. W., Thomas, M. S., Liu, C., Chelton, D. B., Casey, K. S., & Schlax, M. G. (2007). Daily high-resolution blended analyses for sea surface temperature by. *Journal of Climate*, *8*, 1–58. https://doi.org/10.1017/CBO9781107415324.004

Rykaczewski, R. R., & Dunne, J. P. (2010). Enhanced nutrient supply to the California current ecosystem with global warming and increased stratification in an earth system model. *Geophysical Research Letters*, *37*(21), L21606. https://doi.org/10.1029/2010gl045019

Sambe, B., Tandstad, M., Caramelo, A. M., & Brownd, B. E. (2016). Variations in productivity of the Canary current large marine ecosystem and their effects on small pelagic fish stocks. *Environmental Development*, *17*, 105–117. https://doi.org/10.1016/j.envdev.2015.11.012

Santos, A. M. P., Kazmin, A. S., & Peliz, Á. (2005). Decadal changes in the Canary upwelling system as revealed by satellite observations: Their impact on productivity. *Journal of Marine Research*, *63*, 359–379. https://doi.org/10.1357/0022240053693671

Santos, F., DeCastro, M., Gómez-Gesteira, M., & Álvarez, I. (2012). Differences in coastal and oceanic SST warming rates along the Canary upwelling ecosystem from 1982 to 2010. *Continental Shelf Research*, *47*, 1–6. https://doi.org/10.1016/j.csr.2012.07.023

Seabra, R., Varela, R., Santos, A. M., Gómez-Gesteira, M., Meneghesso, C., Wethey, D. S., & Lima, F. P. (2019). Reduced nearshore warming associated with eastern boundary upwelling systems. *Frontiers in Marine Science*, *6*, 1–6. https://doi.org/10.3389/fmars.2019.00104

Signorini, S. R., Franz, B. A., & McClain, C. R. (2015). Chlorophyll variability in the oligotrophic gyres: Mechanisms, seasonality and trends. *Frontiers in Marine Science*, *2*, 1–11. https://doi.org/10.3389/fmars.2015.00001

Smith, S. R., Legler, D. M., & Verzone, K. V. (2001). Quantifying uncertainties in NCEP reanalyses using high-quality research vessel observations. *Journal of Climate*, *14*, 4062–4072. https://doi.org/10.1175/1520-0442(2001)014<4062:QUINRU>2.0.CO;2

Steinacher, M., Joos, F., Frölicher, T. L., Bopp, L., Cadule, P., Cocco, V., et al. (2010). Projected 21st century decrease in marine productivity: A multi-model analysis. *Biogeosciences*, *7*, 979–1005. https://doi.org/10.5194/bg-7-979-2010

Sydeman, W. J., García-Reyes, M., Schoeman, D. S., Rykaczewski, R. R., Thompson, S. A., Black, B. A., & Bograd, S. J. (2014). Climate change and wind intensification in coastal upwelling ecosystems. *Science*, *345*, 77–80. https://doi.org/10.1126/science.1251635

Taboada, F. G., & Anadón, R. (2012). Patterns of change in sea surface temperature in the North Atlantic during the last three decades: Beyond mean trends. *Climatic Change*, *115*, 419–431. https://doi.org/10.1007/s10584-012-0485-6

Timmermans, M., & Marshall, J. (2020). Understanding Arctic Ocean circulation: A review of ocean dynamics in a changing climate. *Journal of Geophysical Research: Oceans*, *125*, e2018JC014378. https://doi.org/10.1029/2018jc014378

Van Camp, L., Nykjaer, L., Mittelstaedt, E., & Schlittenhardt, P. (1991). Upwelling and boundary circulation off Northwest Africa as depicted by infrared and visible satellite observations. *Progress in Oceanography*, *26*, 357–402. https://doi.org/10.1016/0079-6611(91)90012-B

Vantrepotte, V., & Mélin, F. (2009). Temporal variability of 10-year global SeaWiFS time-series of phytoplankton chlorophyll a concentration. *ICES Journal of Marine Science*, *66*, 1547–1556. https://doi.org/10.1093/icesjms/fsp107

Vantrepotte, V., & Mélin, F. (2011). Inter-annual variations in the SeaWiFS global chlorophyll a concentration (1997–2007). *Deep Sea Research Part I: Oceanographic Research Papers*, *58*, 429–441. https://doi.org/10.1016/j.dsr.2011.02.003

Vélez-Belchí, P., Pérez-Hernández, M. D., Casanova-Masjoan, M., Cana, L., & Hernández-Guerra, A. (2017). On the seasonal variability of the Canary Current and the Atlantic meridional overturning circulation. *Journal of Geophysical Research: Oceans*, *122*, 4518–4538. https://doi.org/10.1002/2017jc012774

Verges, A., Steinberg, P. D., Hay, M. E., Poore, A. G. B., Campbell, A. H., Ballesteros, E., & Wilson, S. K. (2014). The tropicalization of temperate marine ecosystems: Climate-mediated changes in herbivory and community phase shifts. *Proceedings of the Royal Society B: Biological Sciences*, *281*, 20140846. https://doi.org/10.1098/rspb.2014.0846

Westberry, T., Behrenfeld, M. J., Siegel, D. A., & Boss, E. (2008). Carbon-based primary productivity modeling with vertically resolved photoacclimation. *Global Biogeochemical Cycles*, *22*, 1–18. https://doi.org/10.1029/2007GB003078

Winton, M., Griffies, S. M., Samuels, B. L., Sarmiento, J. L., & Frölicher, T. L. (2012). Connecting changing ocean circulation with changing climate. *Journal of Climate*, *26*, 2268–2278. https://doi.org/10.1175/jcli-d-12-00296.1

Wooster, W. S., Bakun, A., & McClain, D. R. (1976). The seasonal upwelling cycle along the eastern boundary of the North Atlantic. *Journal of Marine Research*, *34*, 131–141.

Xiu, P., Chai, F., Curchitser, E. N., & Castruccio, F. S. (2018). Future changes in coastal upwelling ecosystems with global warming: The case of the California Current system. *Scientific Reports*, *8*, 2866. https://doi.org/10.1038/s41598-018-21247-7